Supplemental Figure 1

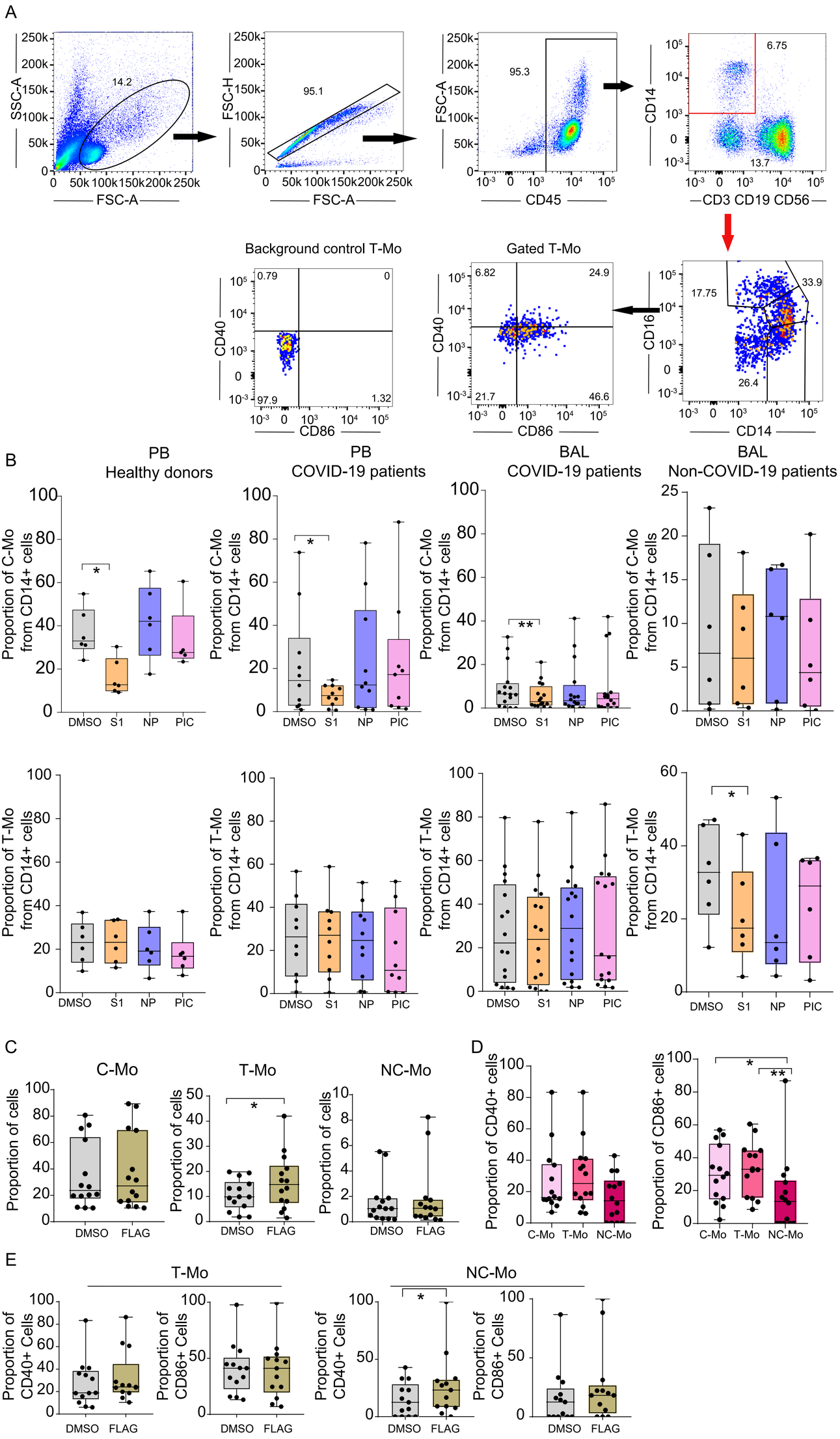

Supplemental Figure 1. Analysis of changes in Mo subsets from PBMC after exposure to SARS-CoV-2 proteins and TLR ligands. (A) Representative flow cytometry gating strategy defining CD14+ CD3-CD19-CD56- Mo from PBMC and identifying Classical (C-Mo), Transitional (T-Mo) and non-classical (NC-Mo) Mo subsets based on differential levels of CD16 and CD14. Levels of CD40 vs CD86 on gated cells from each population were also analyzed. A representative flow cytometry plot on gated T-Mo and the background control for this subset is also shown. (B): Proportions of C-Mo and T-Mo from cultures of bulk PBMC (n=10) and BAL (n=16) from COVID-19 patients, PBMC from healthy donors (n=6) or BAL from non-COVID-19 patients (n=6) in DMSO (grey), S1 peptide (orange), NP peptide (purple) and Poly I:C (PIC, pink) condition. (C): Proportions of C-Mo, T-Mo and NC-Mo in pre-isolated CD14+ Mo (C) after 16h of culture in the presence of DMSO (grey) and flagellin (FLAG, khaki) (n=14). (D) Proportions of CD40+ and CD86+ cells in C-Mo (light pink), T-Mo (pink) and NC-Mo (magenta) populations at baseline conditions in DMSO (n=14). (E): Percentages of CD40+ and CD86+ cells in the indicated Mo subsets on each of the mentioned culture conditions in (C) n=13. Statistical significance was calculated using a two tailed Wilcoxon test: *p<0.05, **p<0.01. Data are represented as box and whiskers with bars representing maximum and minimum values and with median highlighted as a line.

Supplemental Figure 2

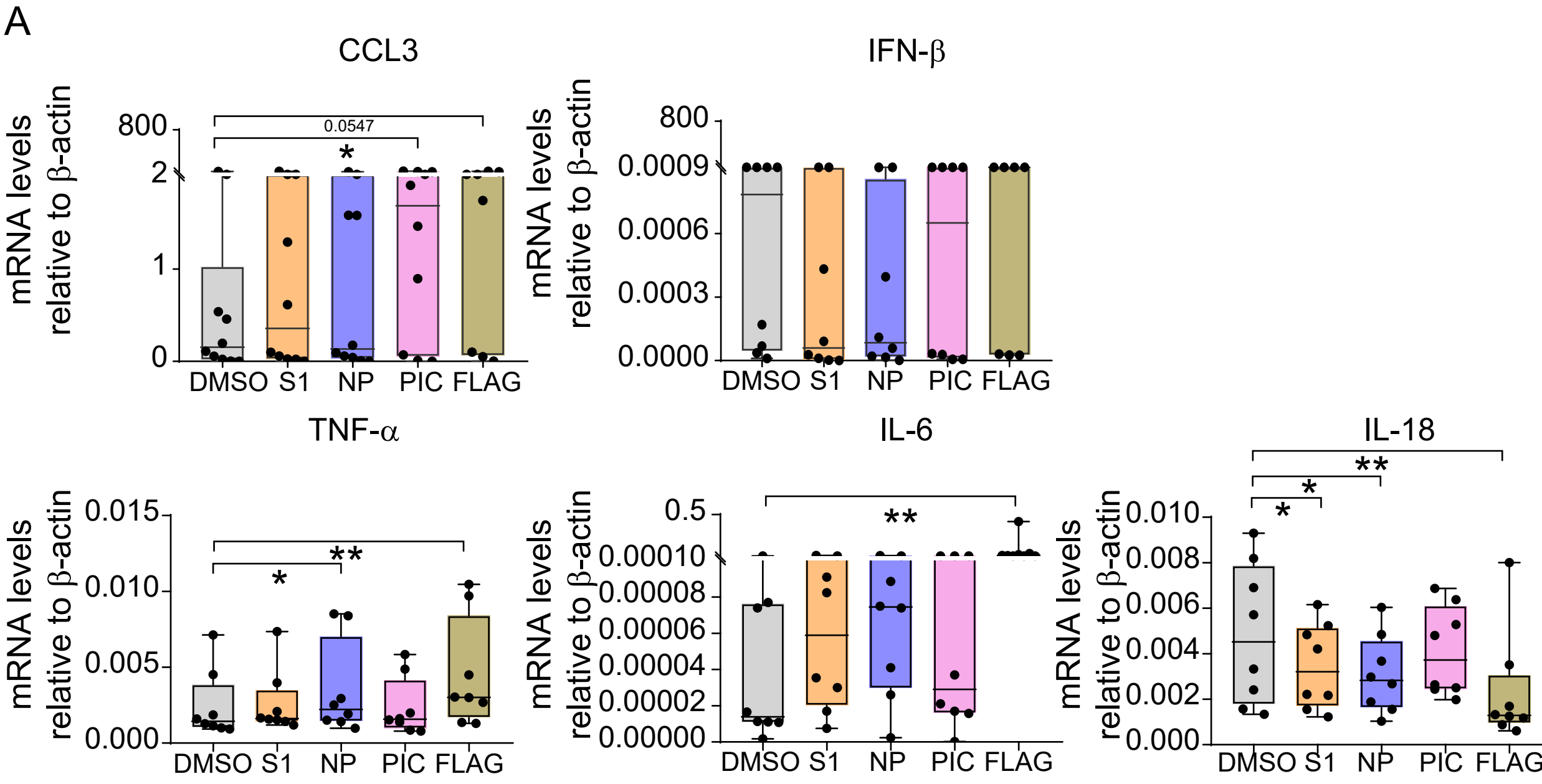

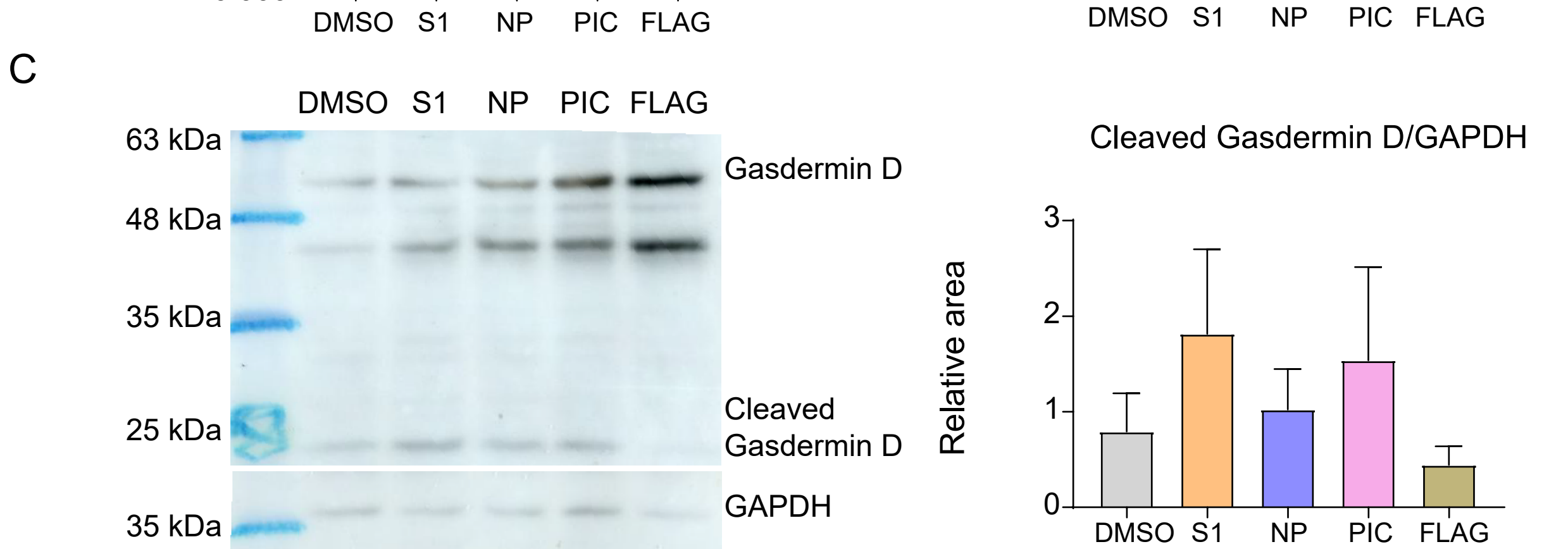

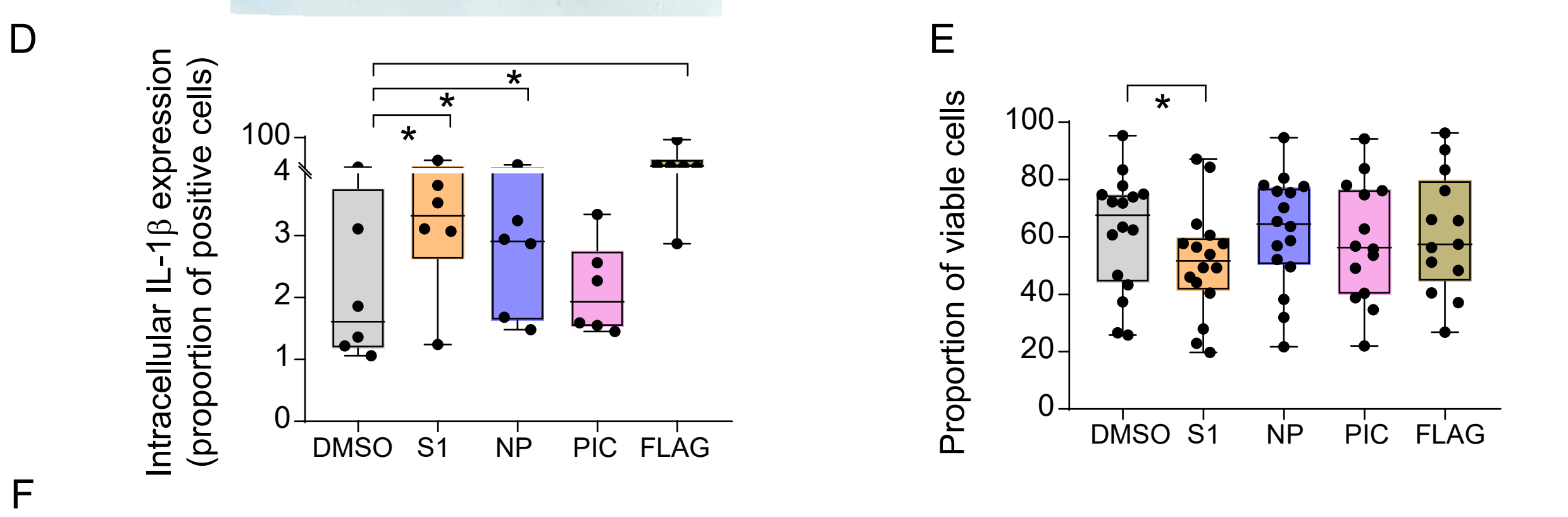

Supplemental Figure 2. Transcriptional levels of proinflammatory cytokines and inflammasome sensors in Mo exposed to SARS-CoV-2 proteins and TLR ligands. (A, B): mRNA levels quantified by RT- qPCR of CCL3 (n=10), IFNβ, TNF-α, IL-6 and IL-18 (n=8) (A) and NLRP3 (n=8) and NLRC4 (n=7) inflammasome sensors (B) in isolated CD14+ Mo cultured in the presence of DMSO or S1 peptide (orange), NP peptide (purple), Poly I:C (PIC, pink), flagellin (FLAG, khaki). Transcriptional levels were normalized to the β-actin expression. (C-F): Representative Western blot analysis of Gasdermin D (C) and IL-1β (F) uncleaved and processed isoforms and GAPDH in Mo cultured in the mentioned conditions. Quantification of results relative to GAPDH from three independent experiments for both proteins is shown on the right. Data in these panels is represented as mean and error bars correspond to SEM. (D, E): Proportions of IL-1β+ (D; n=6) and viable (E; n=16) Mo in the previously mentioned culture conditions. Statistical significance in (A, B, D, E) was calculated using a two tailed Wilcoxon test: *p<0.05, **p<0.01. Data are represented as box and whiskers with bars representing maximum and minimum values and with median highlighted as a line.

Supplemental Figure 3

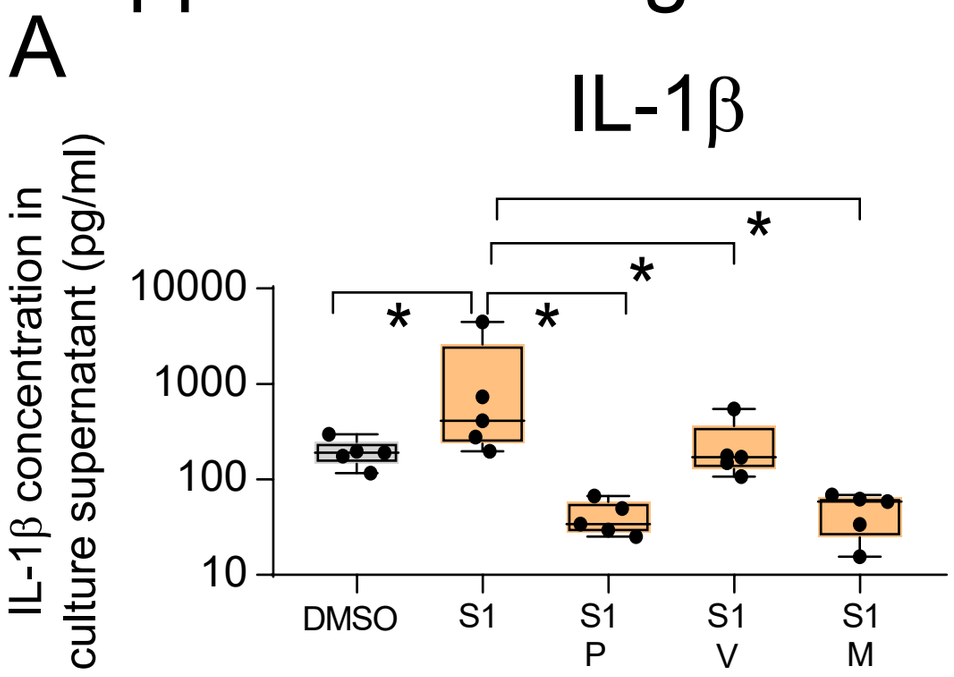

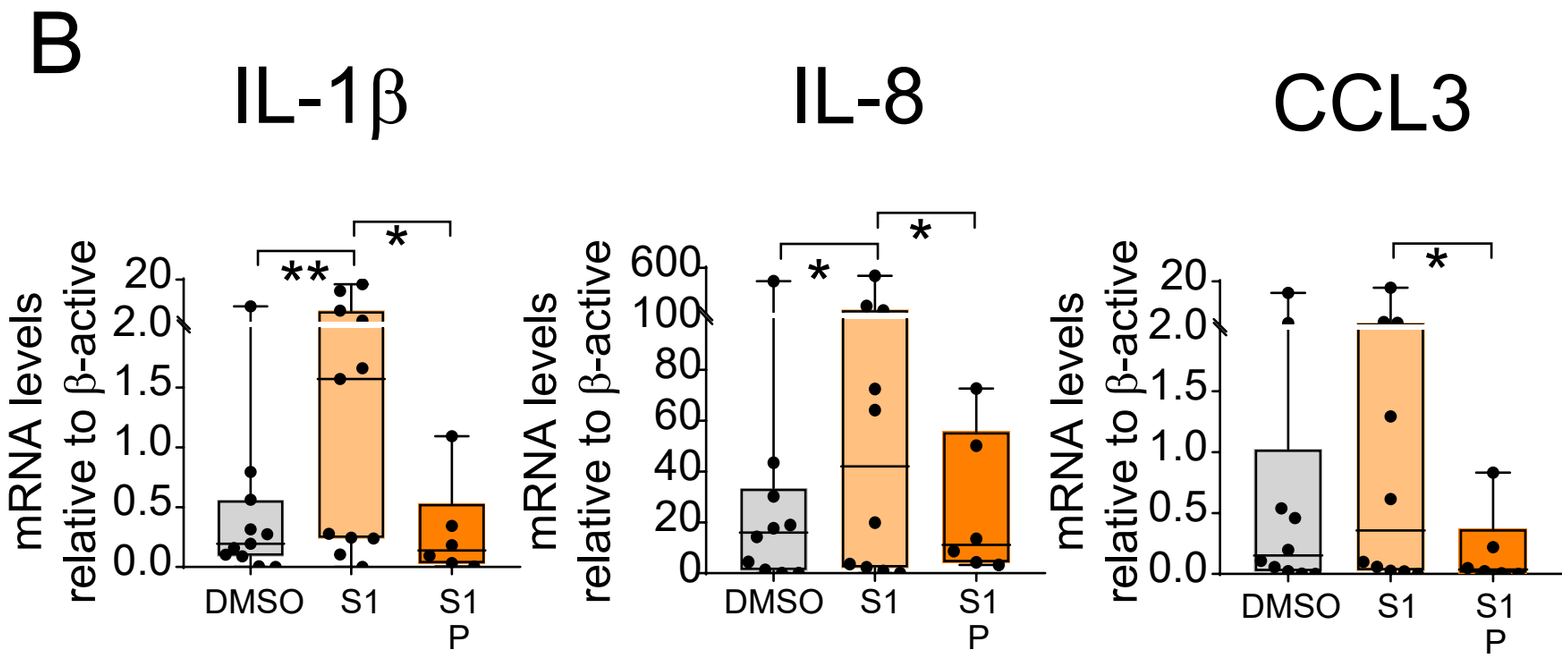

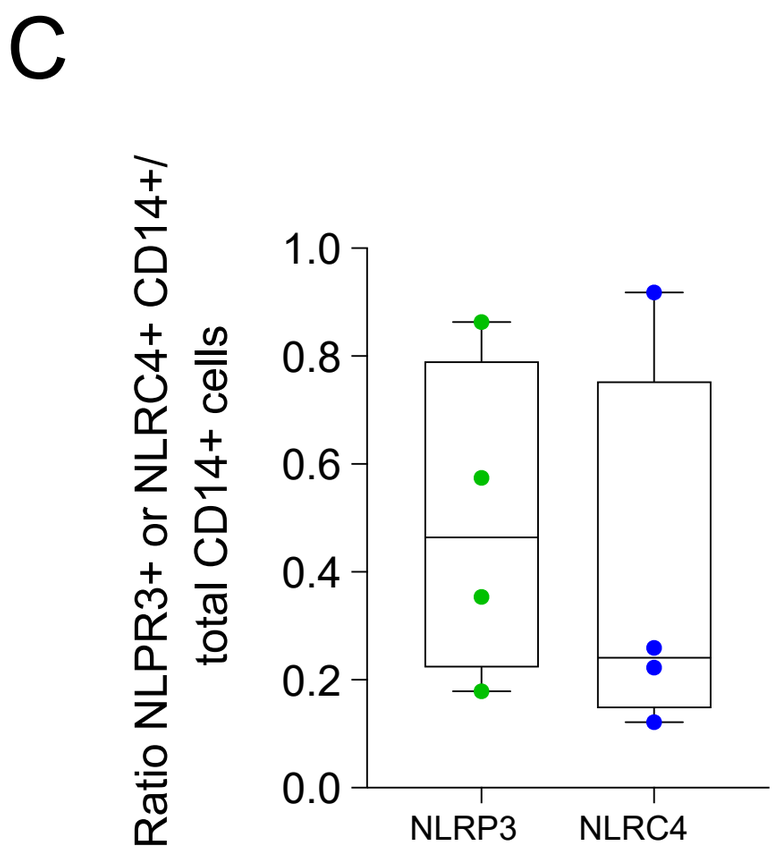

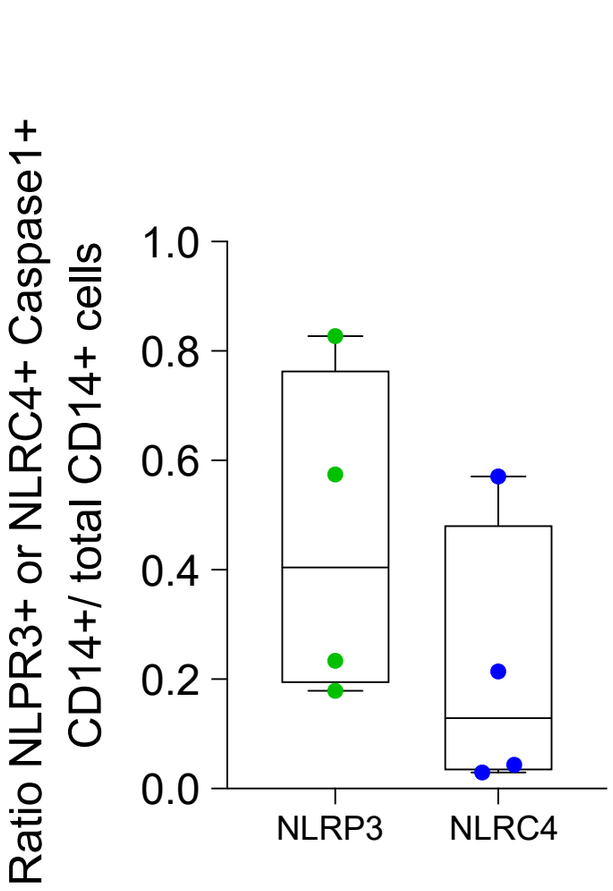

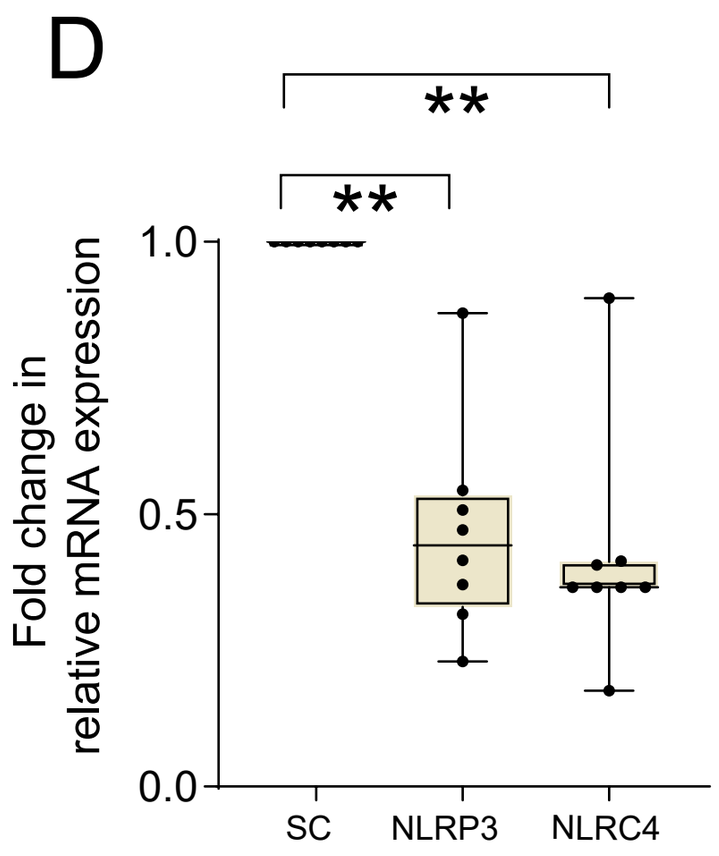

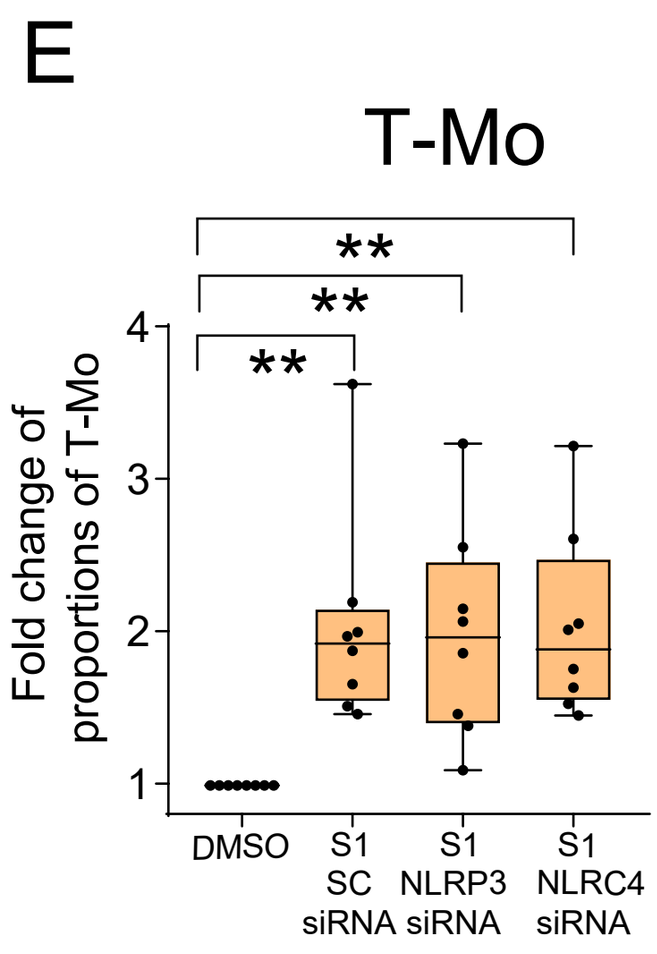

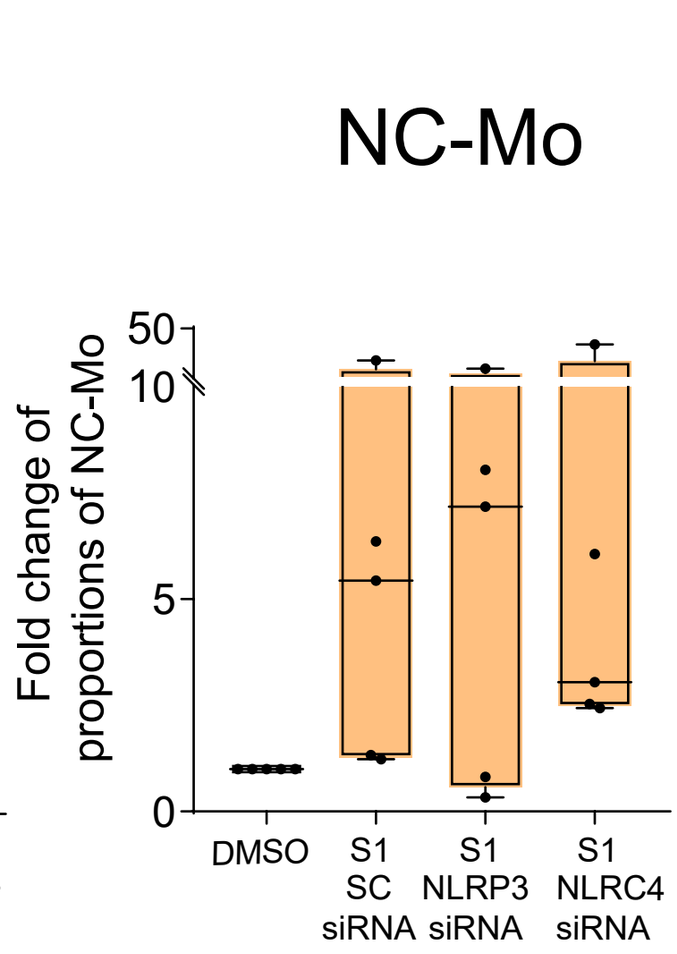

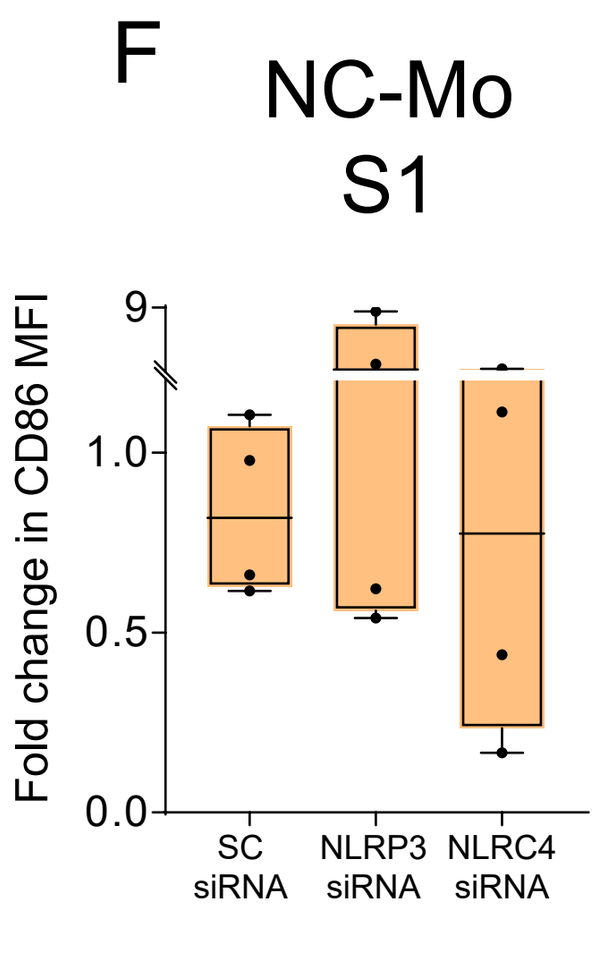

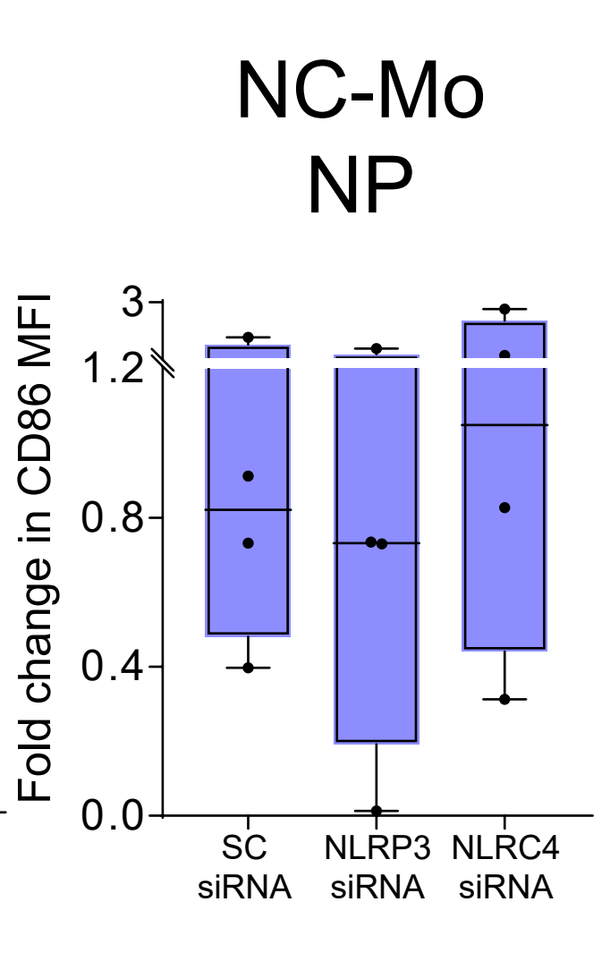

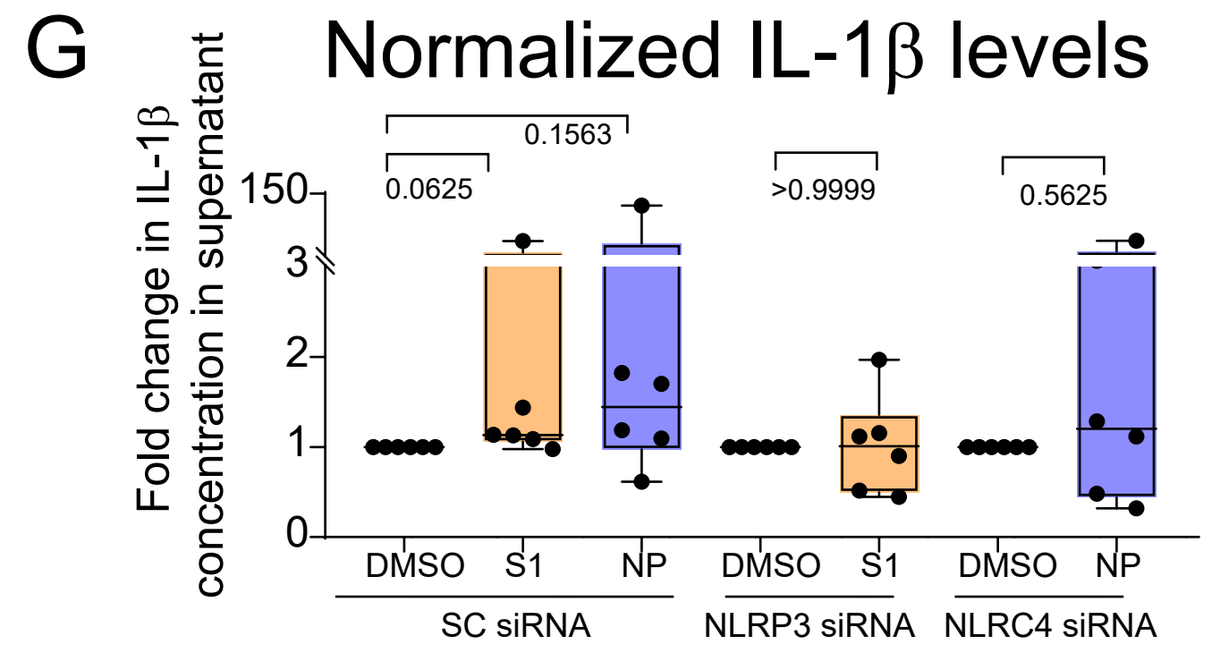

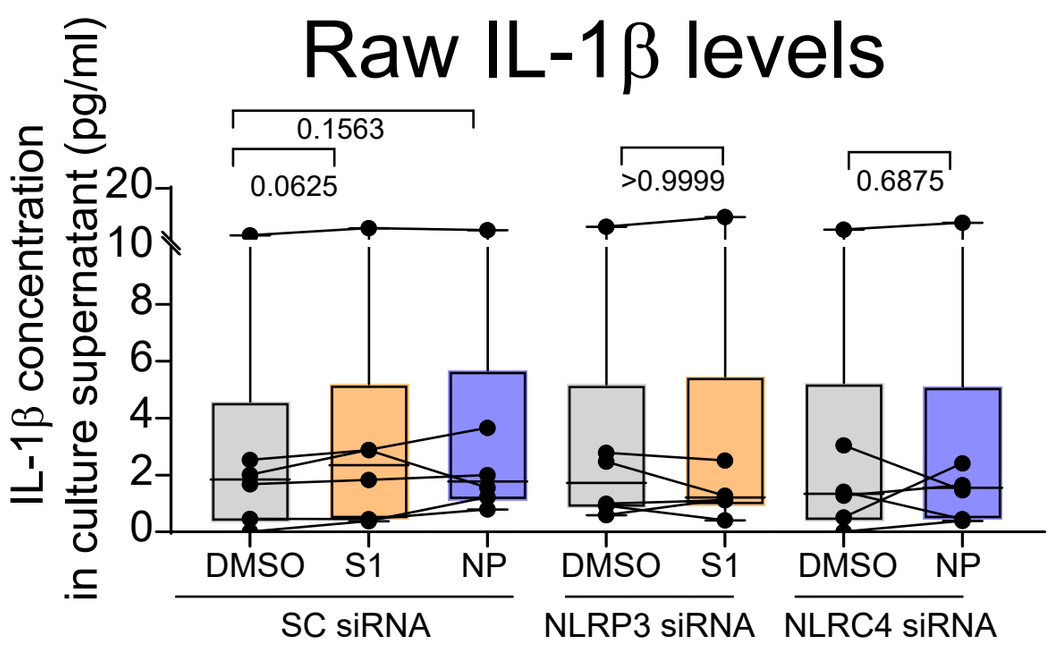

Supplemental Figure 3. Pharmacological and siRNA mediated inhibition of the inflammasome and NFκB. (A): ELISA quantification of the concentrations of secreted IL-1β protein in culture supernatants of Mo cultured in the presence of DMSO (grey) versus S1 (orange) in the presence of DMSO or Parthenolide (P), Z-VAD-FMK (V), and MCC950 (M) (n=5). Statistical significance was calculated using a one-tailed Wilcoxon test *p<0.05. (B) RT-qPCR analysis of IL-1β (n=11), IL-8 (n=10) and CCL3 (n=10) in Mo cultured in the absence or the presence of DMSO (grey), S1with DMSO (orange) or with S1 and Parthenolide (P) (dark orange). (C): Quantification of ratios of cells co-expressing NLRP3 (green) or NLRC4 (blue) with CD14 alone (left) or with caspase 1 (right) from total CD14+ cells in lung tissue from n=3 critical COVID-19 patients. (D): RT-qPCR quantification of NLRP3 and NLRC4 in cells treated with specific siRNAs relative to cells nucleofected with Scramble (SC) siRNAs (n=8). Data are normalized to levels of mRNA in control condition (Scramble) and relative to β-actin expression. (E): Fold change in proportions of T-Mo (n=8) and NC-Mo (n=5) subsets from Mo nucleofected with scramble (SC) siRNA or siRNA specific for NLRP3 and NLRC4 and treated with S1 (orange) compared to DMSO control conditions. (F): Fold change in CD86 MFI on NC-Mo in response to viral proteins (S1 (orange) or NP (purple)) after nucleofection with scramble (SC) or NLRP3 and NLRC4-specific siRNAs (n=4). (G): Impact of nucleofection of Mo with scramble (SC), NLRP3 or NLRC4 specific-siRNAs in levels of secreted IL-1β in supernatants after exposure to S1 and NP compared to DMSO conditions. Normalized and raw data are shown in left and right plots, respectively. Statistical significance of differences for (B, C, D) were calculated using a two-tailed Wilcoxon test *p<0.05, **p<0.01. Data are represented as box and whiskers with bars representing maximum and minimum values and with median highlighted as a line

Supplemental Figure 4

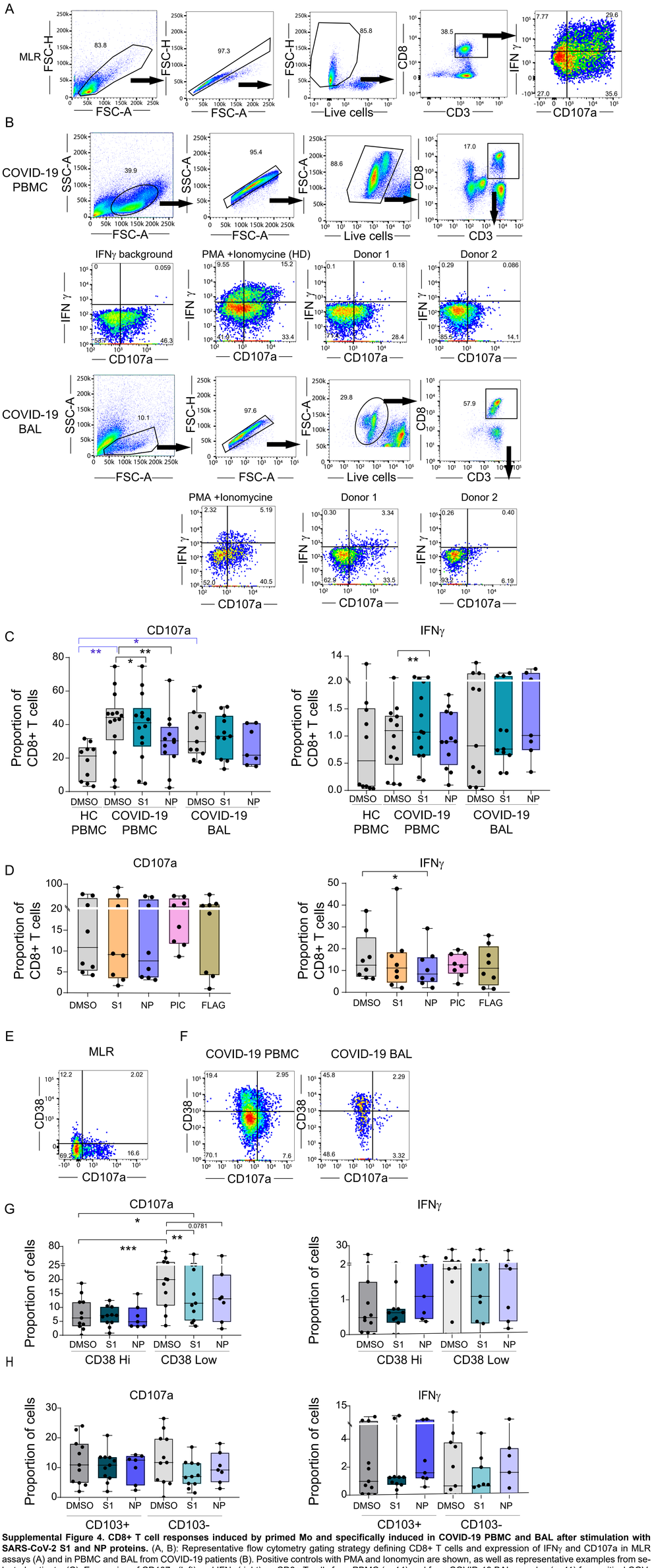

Supplemental Figure 4. CD8+ T cell responses induced by primed Mo and specifically induced in COVID-19 PBMC and BAL after stimulation with SARS-CoV-2 S1 and NP proteins. (A, B): Representative flow cytometry gating strategy defining CD8+ T cells and expression of IFNγ and CD107a in MLR assays (A) and in PBMC and BAL from COVID-19 patients (B). Positive controls with PMA and Ionomycin are shown, as well as representative examples from selected patients. (C): Expression of CD107a (left) and IFNγ (right) on CD8+ T cells from PBMC (n=14) and from COVID-19 BAL samples (n=11) from critical COVID-19 patients at baseline and after stimulation with S1 (green) and NP (purple) peptides or DMSO (grey). Baseline levels from PBMCs obtained from healthy donors cultured in DMSO (grey) are included for comparison purposes (n=10). (D): Proportions CD107a+ and IFNγ+ CD8+ T cells in MLR assays performed in the presence of allogeneic Mo cultured in the presence of DMSO (grey) or S1 (orange), NP (purple), Poly I:C (PIC; pink), Flagellin (FLAG, khaki) and corresponding to normalized data shown in figure 4 (n=8). (E, F): Representative flow cytometry dot plots showing CD38 vs CD107a expression in CD8+ T cells from MLR assays (E) and from COVID-19 BAL and PBMC samples (F). (G, H): Proportions of IFNγ+ and CD107a+ cells in CD38Hi and CD38Low (G) or in CD103+ and CD103- (H) CD8+ T cells from BAL exposed to DMSO (dark grey, grey) o SARS-CoV-2 S1 (dark green, green) or NP (blue, light purple) (n=11). A Mann-Whitney test was used to statistical differences between samples from different cohorts. Statistical differences between different experimental conditions in the same groups were calculated using a two-tailed Wilcoxon matched pairs test *p<0.05, **p<0.01, ***p<0.001. Data are represented as box and whiskers with bars representing maximum and minimum values and with median highlighted as a line.

Supplemental Figure 5

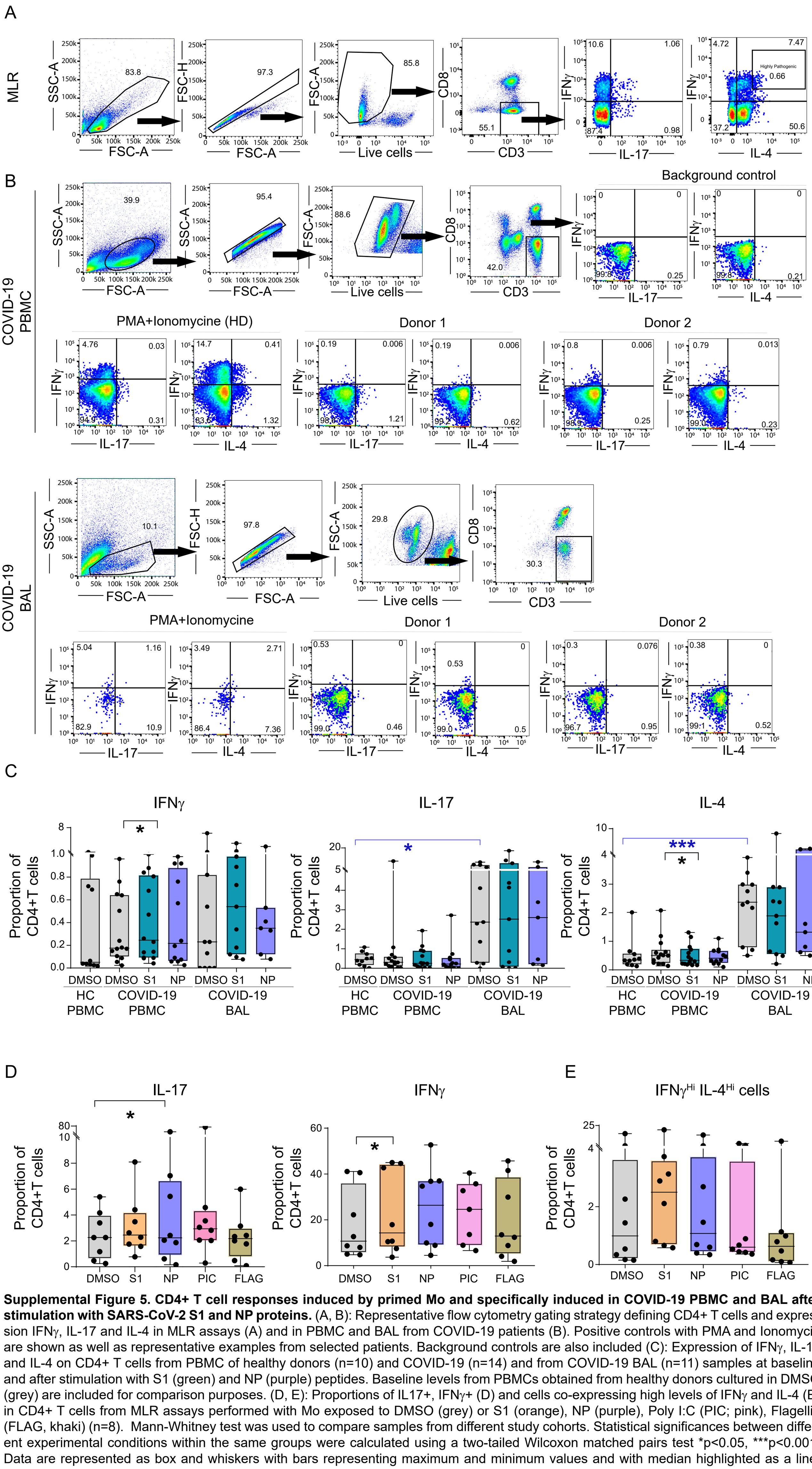

Supplemental Figure 5. CD4+ T cell responses induced by primed Mo and specifically induced in COVID-19 PBMC and BAL after stimulation with SARS-CoV-2 S1 and NP proteins. (A, B): Representative flow cytometry gating strategy defining CD4+ T cells and expression IFNγ, IL-17 and IL-4 in MLR assays (A) and in PBMC and BAL from COVID-19 patients (B). Positive controls with PMA and Ionomycin are shown as well as representative examples from selected patients. Background controls are also included (C): Expression of IFNγ, IL-17 and IL-4 on CD4+ T cells from PBMC of healthy donors (n=10) and COVID-19 (n=14) and from COVID-19 BAL (n=11) samples at baseline and after stimulation with S1 (green) and NP (purple) peptides. Baseline levels from PBMCs obtained from healthy donors cultured in DMSO (grey) are included for comparison purposes. (D, E): Proportions of IL17+, IFNγ+ (D) and cells co-expressing high levels of IFNγ and IL-4 (E) in CD4+ T cells from MLR assays performed with Mo exposed to DMSO (grey) or S1 (orange), NP (purple), Poly I:C (PIC; pink), Flagellin (FLAG, khaki) (n=8). Mann-Whitney test was used to compare samples from different study cohorts. Statistical significances between different experimental conditions within the same groups were calculated using a two-tailed Wilcoxon matched pairs test *p<0.05, ***p<0.001. Data are represented as box and whiskers with bars representing maximum and minimum values and with median highlighted as a line.

Supplemental figure 6

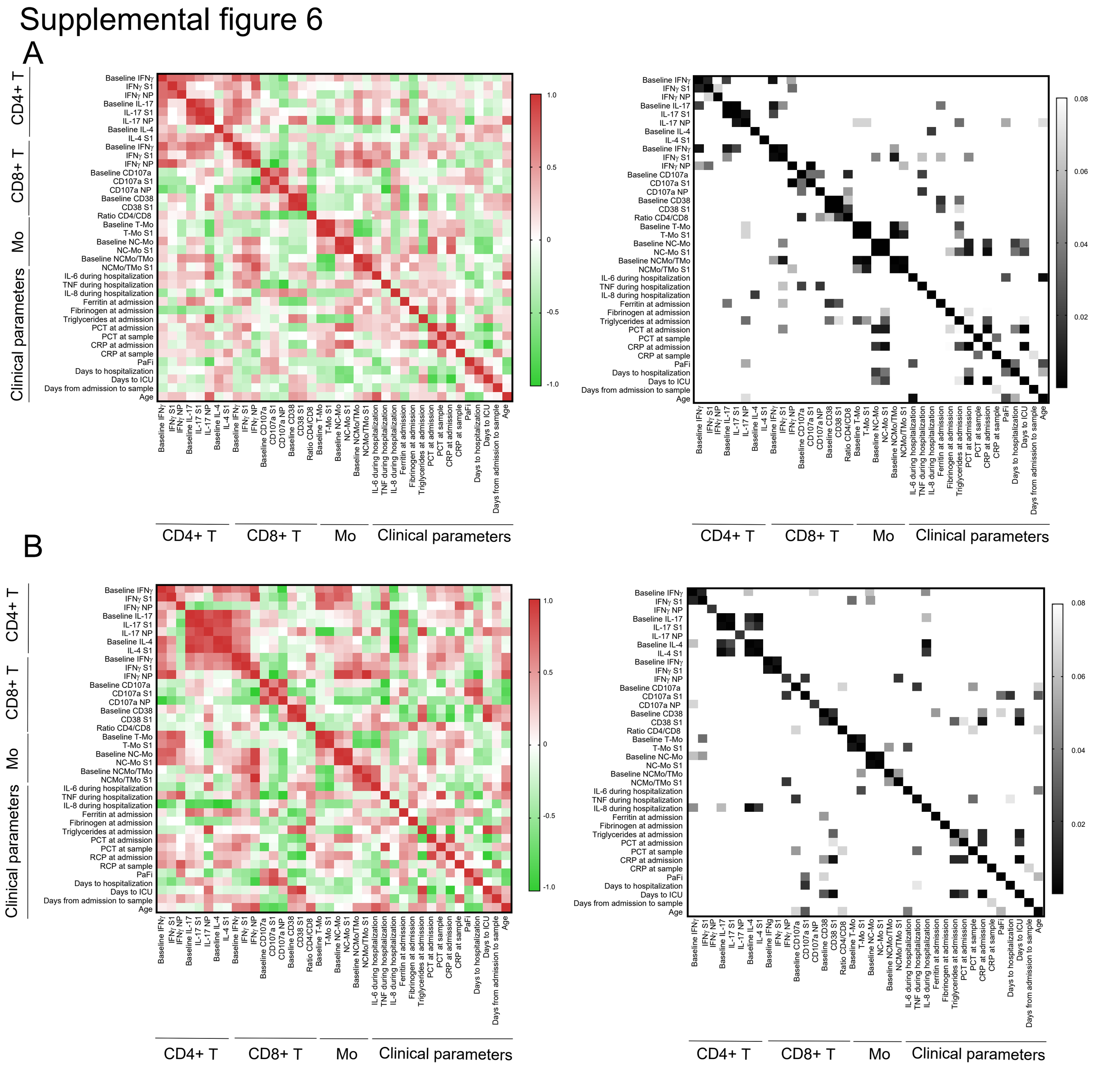

Supplemental Figure 6. Correlation networks between Mo, T cell and clinical patterns in BAL from critical COVID-19 patients. (A, B): Heatmaps showing spearman correlation networks of the indicated Mo subsets, CD4+ and CD8+ T cell responses present at baseline or after SARS-CoV-2 peptide stimulation in all BAL samples from COVID-19 patients tested (A) n=12 or exclusively those in which IL-17 induction was observed in response to SARS-CoV-2 S1 or NP peptide stimulation (B) n=7. Heatmaps of the left show colors representing positive (red) or negative (green) R values of association. Heatmaps on the right show levels of statistical significance for the same corresponding networks. (C, D) Proportions of IFNγ+ (left, C and D) and IL-17+ (C) or CD107a+ (D) (right) CD4+ and CD8+ T cells after culture with allogeneic Mo treated with either Scramble, NLRP3 or NLRC4 specific siRNAs and in the absence (DMSO) or presence of S1 (orange) or NP (purple) stimulation (n=4). Data are represented as box and whiskers with bars representing maximum and minimum values and with median highlighted as a line.

Number of PB samples	n=17	
Age *median (min-max)*	69 (44-78)	
Sex male *n (%)*	12 (71)	
Days since symptoms to admission *median (min-max)*	4.5 (0-25)	
Days since admission to sample *median (min-max)*	26 (5-47)	
Days since admission to ICU *median (min-max)*	6 (0-19)	
Admission to ICU *n (%)*	17 (100)	
Comorbidities *n (%)*		
Arterial hypertension	9 (53)	
Diabetes mellitus	5 (29)	
Dyslipidemia	7 (41)	
Lung disease	1 (6)	
Analytics parameters *median (min-max)*		
$PaFiO_2$ (PaO2/FiO2)	146 (60-367)	
PCT at sample collection (ng/ml)	0.3 (0.06-2.87)	
PCT at admission (ng/ml)	0.16 (0.07-1)	
Lymphocytes miles/mm^3	850 (420-5450)	
LDH (U/L)	288 (145-548)	
D-DIMER (µg/ml)	2.2 (1.33-14.7)	
CRP at sample collection (mg/dl)	9 (0.13-20.8)	
CRP at admission (mg/dl)	7.3 (3.4-24)	
GGT (U/l)	201.5 (25-473)	
Glucose (mg/dl)	152 (87-207)	
Ferritin at admission (ng/ml)	712 (114-2733)	
Triglycerides at admission (mg/dl)	271 (43-674)	
Fibrinogen at admission (mg/dl)	641 (389-1152)	
IL-6 (pg/ml)	31 (2-56)	
Exitus *n (%)*	7 (41)	
Superinfection *n (%)*		
Bacterial	8 (47)	
Fungal	7 (41)	
Both	5 (29)	
Treatment *n (%)*		
Antibiotics	11 (65)	
Glucocorticoids	13 (76)	
Biologics	6 (35)	
Antiviral	0 (0)	

Supplemental table 1. Peripheral blood samples from COVID-19 patients used in the study.

Number of Samples	N=17
Age *median (min-max)*	69 (44-78)
Sex male *n (%)*	12 (71)
Days since symptoms to admission *median (min-max)*	4.5 (0-25)
Days since admission to sample *median (min-max)*	26 (5-47)
Days since admission to ICU *median (min-max)*	6 (0-19)
Admission to ICU *n (%)*	17 (100)
Comorbidities *n (%)*	
Arterial hypertension	10 (59)
Diabetes mellitus	6 (35)
Dyslipidemia	11 (65)
Lung disease	1 (6)
Analytics parameters *median (min-max)*	
$PaFiO_2$ (PaO2/FiO2)	158 (94.3-211.3)
PCT at sample collection (ng/ml)	0.3 (0.09-1.68)
PCT at admission (ng/ml)	0.13 (0.04-1.01)
Lymphocytes miles/mm^3	780 (50-5450)
LDH (U/L)	284 (145-426)
D-DIMER (µg/ml)	2.07 (1.09-14.7)
CRP at sample collection (mg/dl)	9.6 (0.81-20.78)
CRP at admission (mg/dl)	7.3 (3.4-24)
GGT (U/l)	131 (25-473)
Glucose (mg/dl)	153 (92-207)
Ferritin at admission (ng/ml)	934 (313-2733)
Triglycerides at admission (mg/dl)	137 (43-451)
Fibrinogen at admission (mg/dl)	688 (540-952)
IL-6 (pg/ml)	27.65 (2-56)
Exitus *n (%)*	7 (41)
Superinfection *n (%)*	
Bacterial	11 (65)
Fungal	7 (41)
Both	6 (35)
Treatment *n (%)*	
Antibiotics	12 (71)
Glucocorticoids	17 (100)
Biologics	6 (35)
Antiviral	1 (6)

Supplemental table 2. Bronchoalveolar lavage samples from COVID-19 patients used in the study.

Number of Non-COVID-19 BAL samples	n=6
Age median (min-max)	69 (38-77)
Pathologies	
Cancer n (%)	3 (50)
Intersticial lung disease (ILD) n (%)	3 (50)

Supplemental table 3. Parameters of Non-COVID-19 patients whose BAL samples were used in the study

Antibody	Fluorochrome	Provider	Dilution	Clone	Ref.
CD14	PE	BioLegend	1:50	63D3	367104
CD14	APC-Cy7	BD	1:50	MφP9	557831
CD16	PB	BioLegend	1:50	3G8	302032
CD40	FITC	BioLegend	1:50	5C3	334306
CD86	PeCy7	BioLegend	1:50	BU63	374210
CD3	PB	Immunostep	1:50	33-2A3	3CFB1-100T
CD107a	APC	BioLegend	1:300	H4A3	328620
CD107a	BV510	BioLegend	1:200	H4A3	328631
CD38	PeCy7	BioLegend	1:50	HB-7	356608
CD45	V500	BD	1:50	HI30	560777
CD1c	PE	BD	1:50	F10/21A3	564900
CD19	PercP/Cyanine5.5	BioLegend	1:50	SJ25C1	363016
CD56	PercP/Cyanine5.5	BioLegend	1:50	5.1H11	362506
CD3	PercP/Cyanine5.5	BioLegend	1:50	HIT3a	300328
IL-1β	FITC	BioLegend	1:100	H1b-98	511705
HLA-DR	APC	BioLegend	1:50	3D12	342606
IL-17	PE	BioLegend	1:100	BL168	512306
IL-17	APC	Invitrogen	1:100	eBio64DEC17	17-7179-42
IL-4	PE	BD	1:30	340451	340451
IL-4	APC	BD	1:100	MP4-25D2	554486
CXCR5	PE	BioLegend	1:50	42D1	338705
CD8	PercP	BioLegend	1:50	HIT8a	300922
IFNγ	BV605	BioLegend	1:50	B27	506542
IFNγ	FITC	BD	1:100	4S.B3	554551
CD103	BV711	BioLegend	1:50	Ber-ACT8	350222

Supplemental table 4. List of antibodies used for Flow cytometry analysis in the study.

Specifitiy	Species Origin	Reactivity	Provider	Clone	Ref.
NLRC4	Rabbit	Human	abcam	Polyclonal	ab115537
IFNγ	Rabbit	Human	abcam	EPR21704	ab231036
CD14	Mouse	Human	abcam	4B4F12	ab182032
NLRP3	Rabbit	Human	Cell Siganling	D4D8T	15101
IL-17	Goat	Human	RyD Systems	Polyclonal	AF-317-SP
Caspase-1	Goat	Human	RyD Systems	Polyclonal	AF6215
CD3	Rabit	Human	Dako	F7.2.38	M7254
IgG	Donkey	Rabbit	Invitrogen	Polyclonal	A-21206
IgG	Donkey	Goat	Invitrogen	Polyclonal	A-11057
IgG	Donkey	Mouse	Invitrogen	Polyclonal	A-31571

Supplemental Table 5. List of antibodies used for Immunohistochemistry in the study.

	Survivors (n=6)	Exitus (n=6)	*p*-value
NC Mo at baseline	17.2 (11.1-22.4)	7.8 (1.8-9.4)	0.05
NC Mo after S1	30.3 (9.3-30.6)	9.8 (3.8-15.4)	0.08
NC Mo after NP	20.5 (12.8-25.6)	5.5 (3.2-9.6)	0.02
IL-4 at baseline	0.8 (0.7-2.4)	2.9 (2.3-3.4)	0.04

NC Mo: non-classical monocytes. NP: nucleoprotein.

Data are shown as median (interquartile range). Non-parametric Mann-Whitney tests were used to assess statistical significance. $p<0.05$ was considered as statistically significant.

	No superinfection (n=5)	Bacterial superinfection (n=3)	Bacterial and fungal superinfection (n=4)	*p*-value	Post-hoc Dunn's test
CD4 IL-17 at baseline	2.4 (2.3-6.4)	0.2 (0-1.4)	7.1 (5.1-9)	0.03	Bacterial and fungal>bacterial
CD4 IL-17 after S1	4.1 (2.5-4.4)	0 (0-0.1)	10.1 (5-14.6)	0.02	Bacterial and fungal>bacterial; no superinfection> bacterial
CD4 IL-17 after NP	2.6 (0.2-3.4)	0.3 (0.2-0.5)	8.2 (6.3-10)	0.1	_____

NP: nucleoprotein.

Data are shown as median (interquartile range). Non-parametric Kruskal-Wallis tests followed by post-hoc Dunn's tests were used to assess statistical significance. $p<0.05$ was considered as statistically significant.

Supplemental Table 6. Statistical analysis of COVID-19 patients distribution based on survival and bacterial or fungal superinfection.

Molecular weight control: BlueStar Plus Prestained Protein Marker (Nippon Genetics)

Phosphorylated p65, total p65 and GAPDH included in Main figure 2B analysis

Chemiluminiscence+Marker

Chemiluminiscence

DMSO S1 NP PIC FLAG

75 kDa
63 kDa

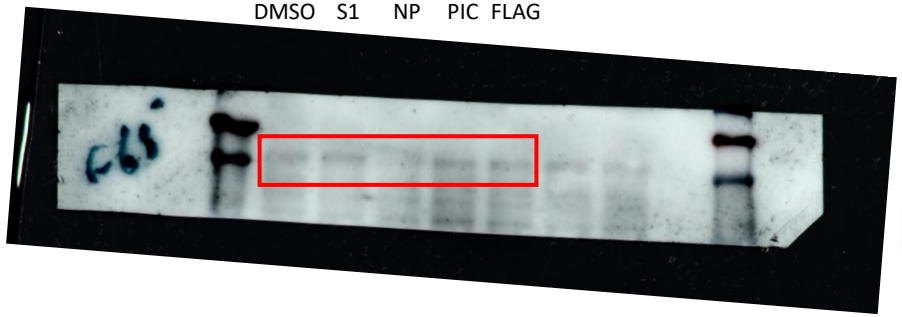

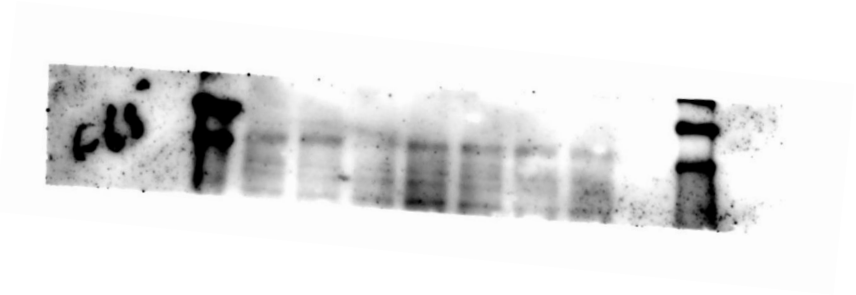

Phosphorylated p65 (65 kDA)
(Cell Signaling 3039)

DMSO S1 NP PIC FLAG

75 kDa
63 kDa

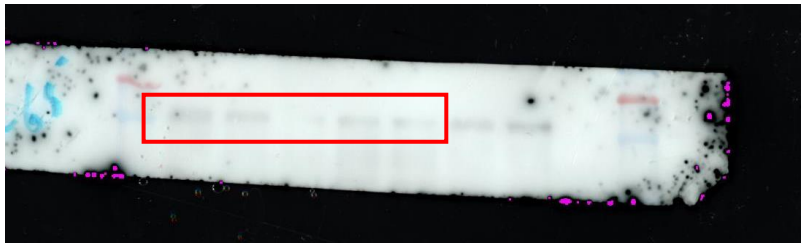

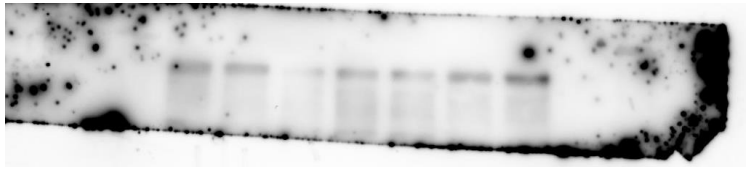

Total p65 (65 kDA)
(Abcam E379; ab32536)

DMSO S1 NP PIC FLAG

48 kDa
35 kDa
25 kDa
20 kDa
17 kDa
11 kDa

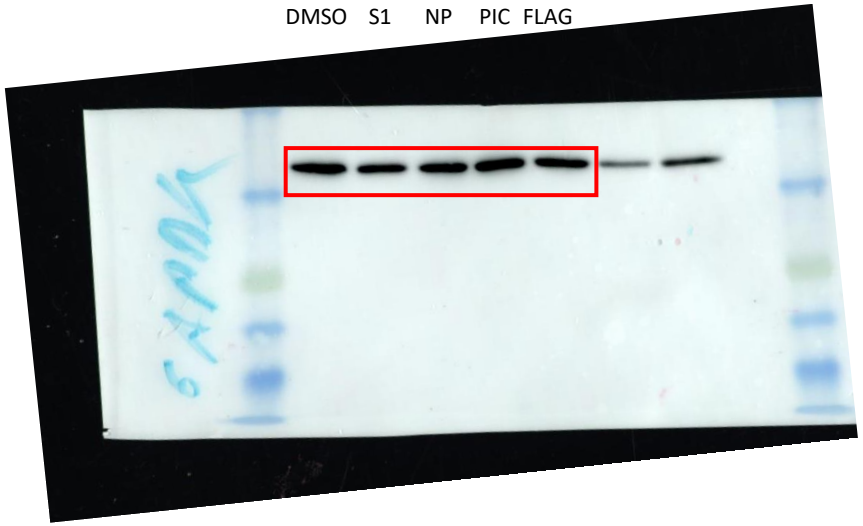

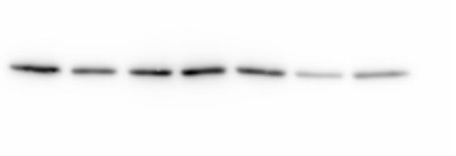

GAPDH (35 kDa)
(FF26A/F9 BioLegend)

Chemiluminiscence+Marker

Chemiluminiscence

Phosphorylated p65, total p65 and GAPDH included in Main figure 2B analysis

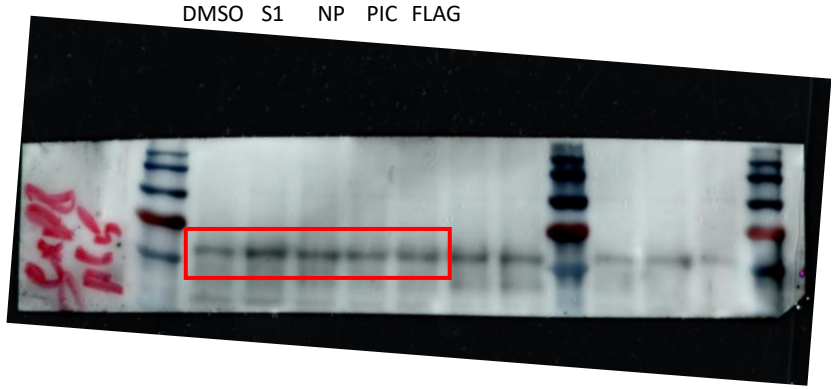

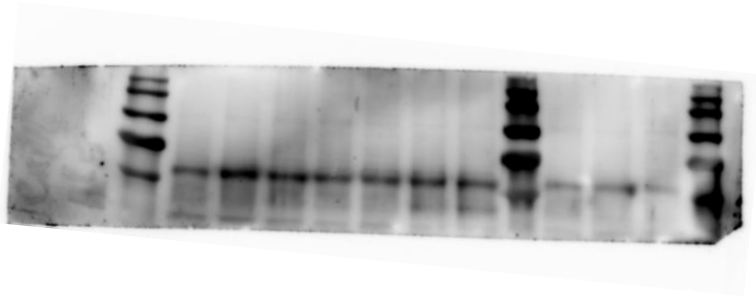

Phosphorylated p65 (65 kDA)
(Cell Signaling 3039)

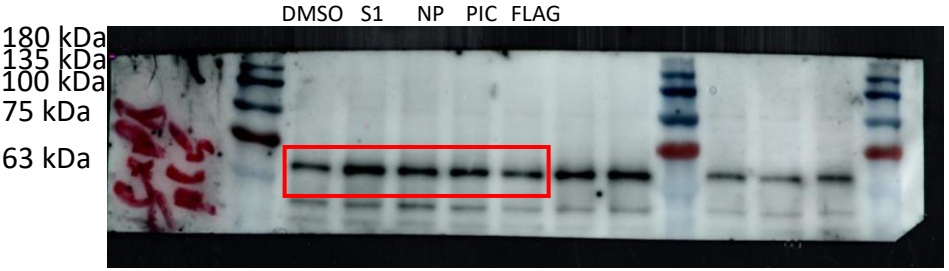

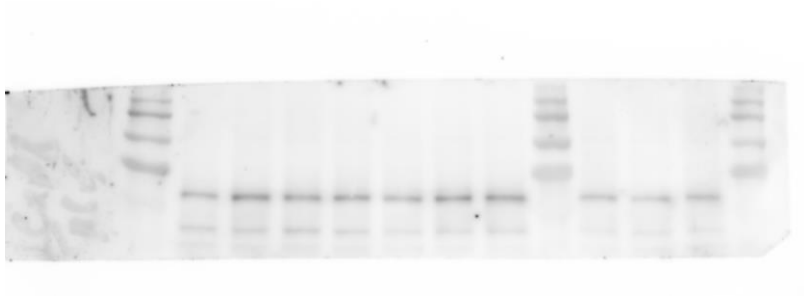

Total p65 (65 kDA)
(Abcam E379; ab32536)

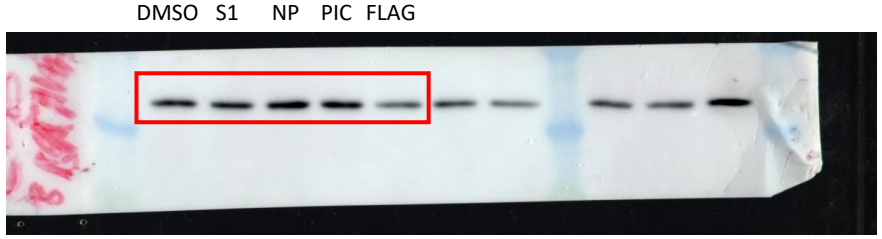

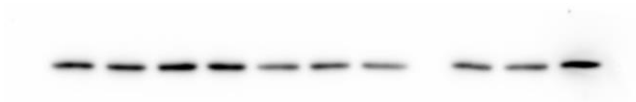

GAPDH (35 kDa)
(FF26A/F9 BioLegend)

Chemiluminiscence+Marker

Chemiluminiscence

Phosphorylated p65, total p65 and GAPDH included in Main figure 2B analysis

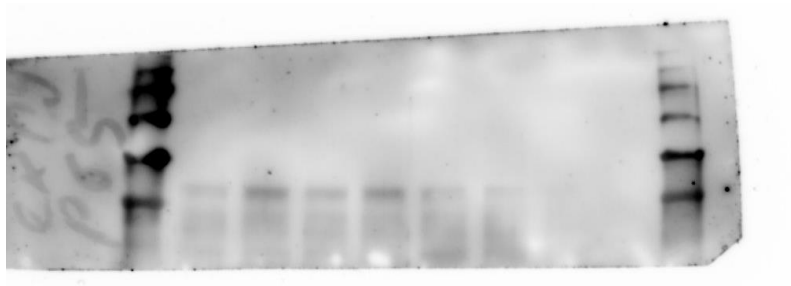

Phosphorylated p65 (65 kDA)
(Cell Signaling 3039)

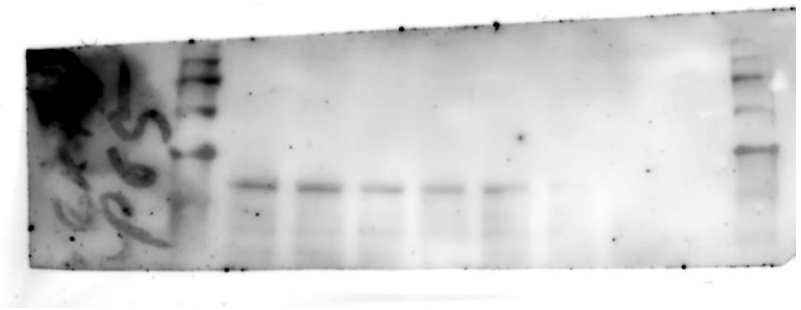

Total p65 (65 kDA)
(Abcam E379; ab32536)

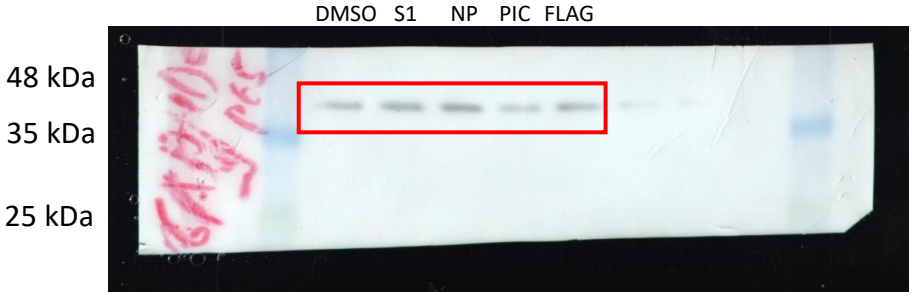

GAPDH (35 kDa)
(FF26A/F9 BioLegend)

Chemiluminiscence+Marker

Chemiluminiscence

Phosphorylated p65, total p65 and GAPDH included in Main figure 2B analysis

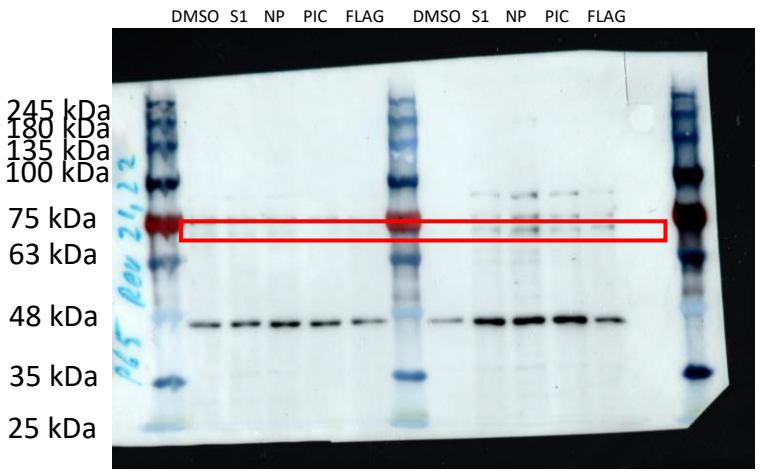

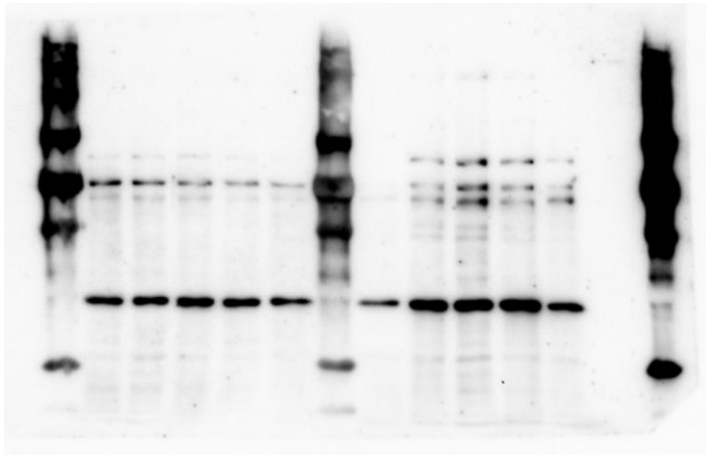

Phosphorylated p65 (65 kDA)
(Cell Signaling 3039)

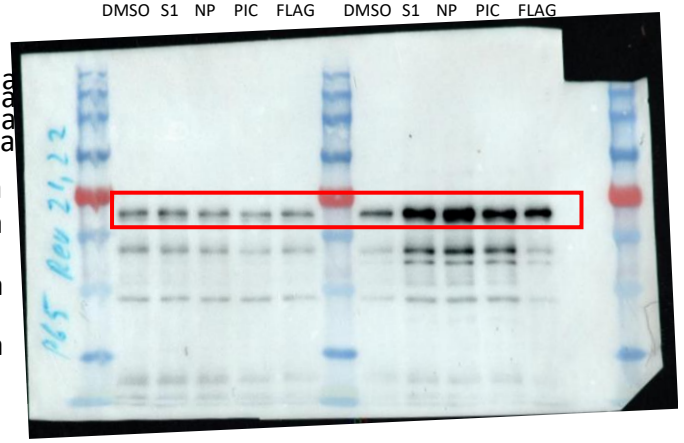

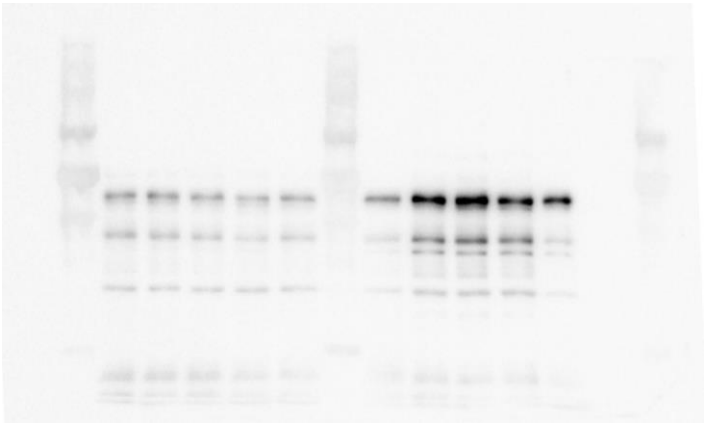

Total p65 (65 kDA)
(Abcam E379; ab32536)

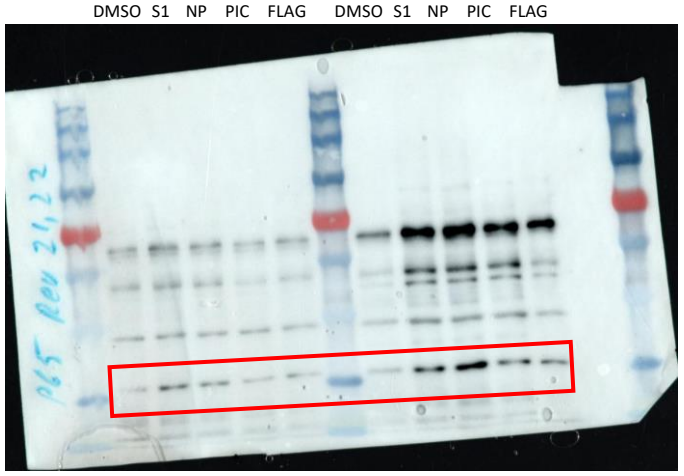

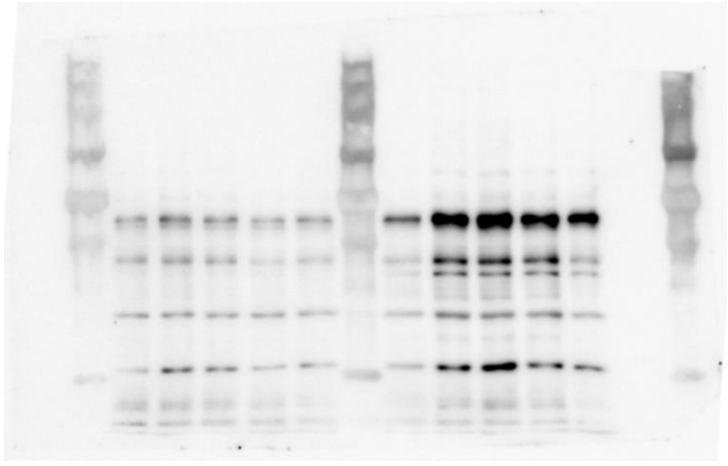

GAPDH (35 kDa)
(FF26A/F9 BioLegend)

Chemiluminiscence+Marker

Chemiluminiscence

Caspase-1 and GAPDH included in Main figure 2C analysis

S1 DMSO

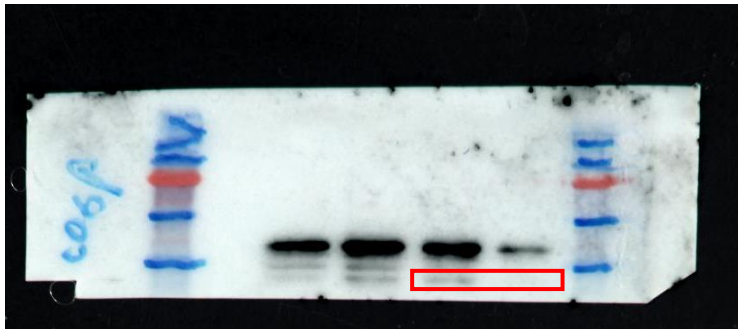

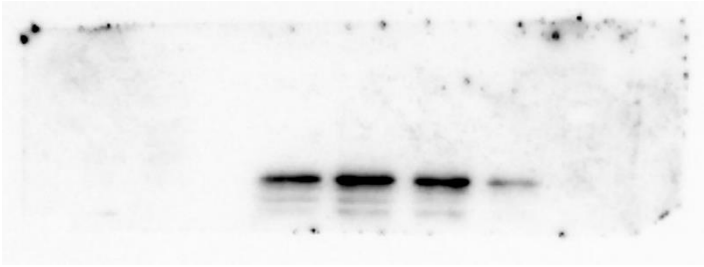

Cleaved Caspase-1 (52 kDa) (AF6215; R&D Systems)

S1 DMSO

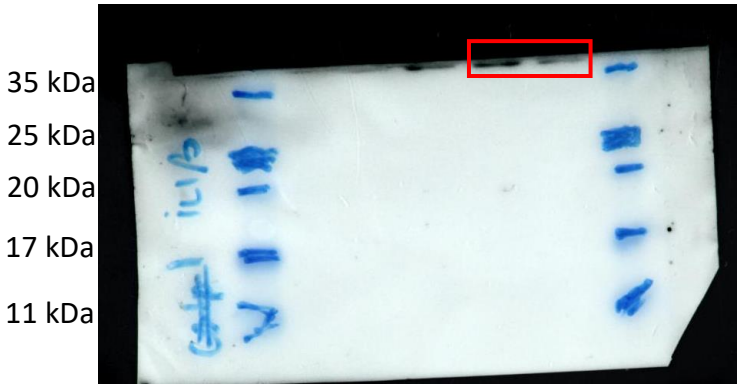

GAPDH (35 kDa) (FF26A/F9 BioLegend)

Chemiluminiscence+Marker

DMSO S1 NP PIC FLAG

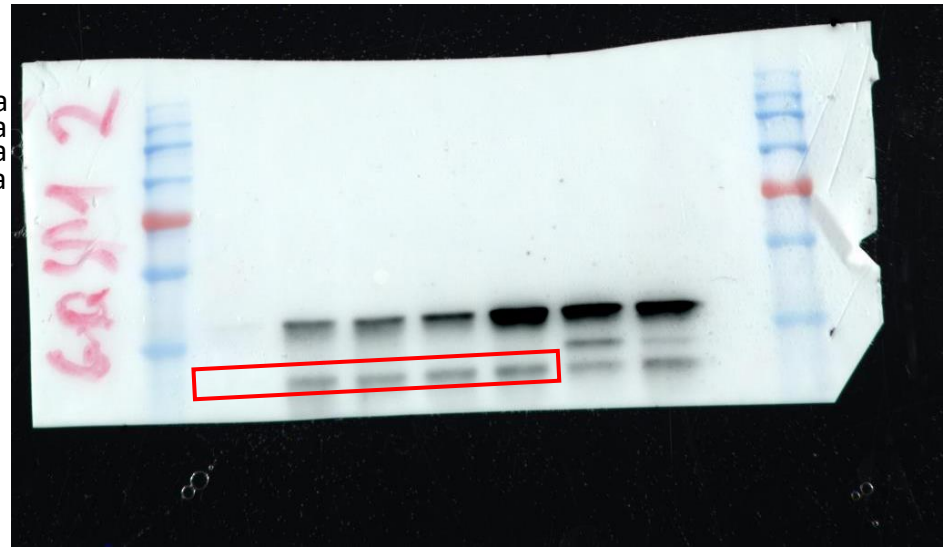

DMSO S1 NP PIC FLAG

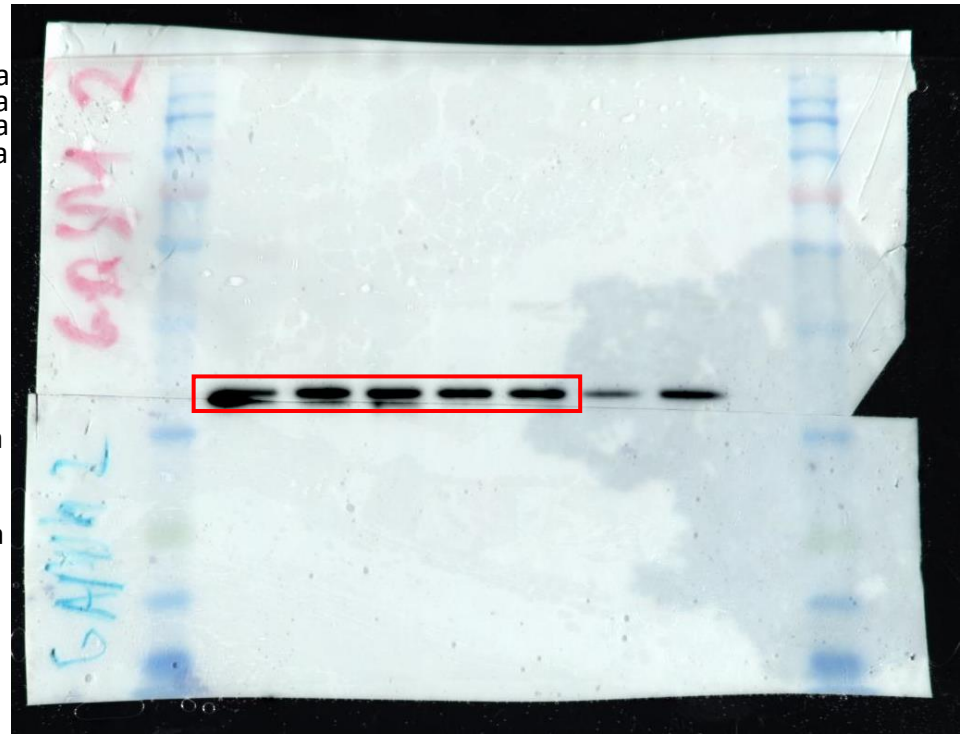

Chemiluminiscence

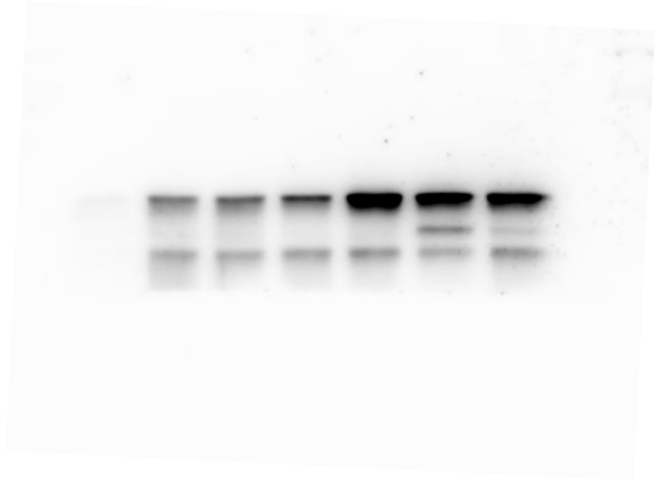

Cleaved Caspase-1 (52 kDa) (AF6215; R&D Systems)

GAPDH (35 kDa) (FF26A/F9 BioLegend)

Caspase-1 and GAPDH included in Main figure 2C analysis

Chemiluminiscence+Marker

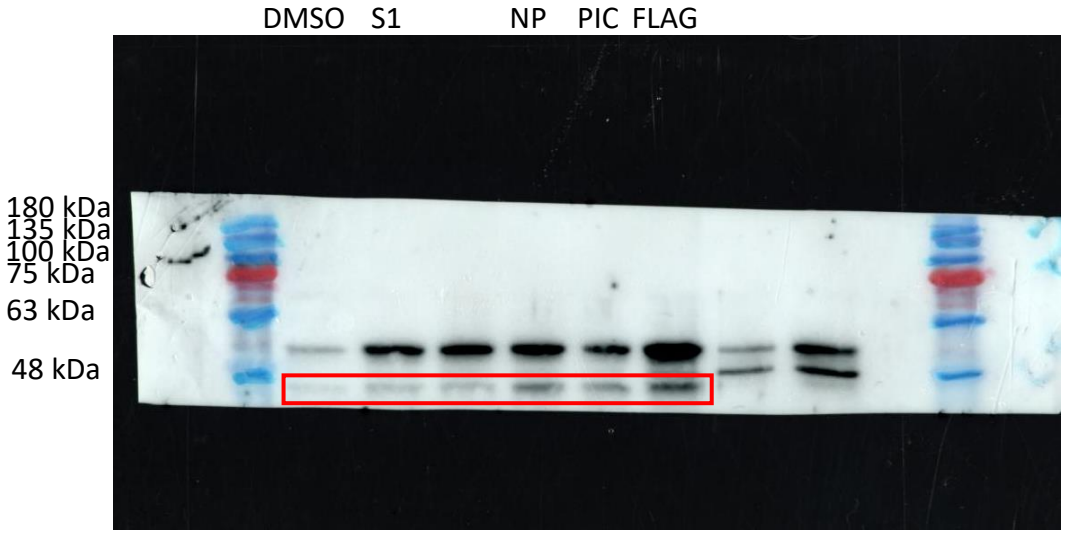

Chemiluminiscence

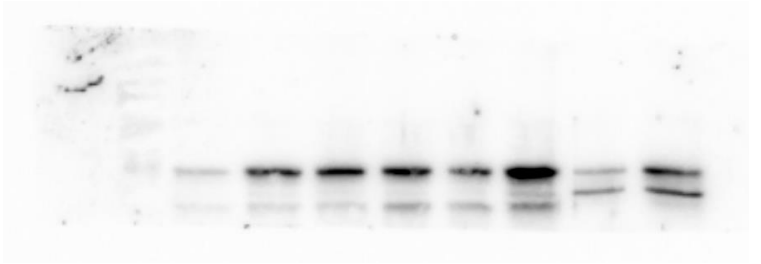

Caspase-1 and GAPDH included in Main figure 2C analysis

Cleaved Caspase-1 (52 kDa) (AF6215; R&D Systems)

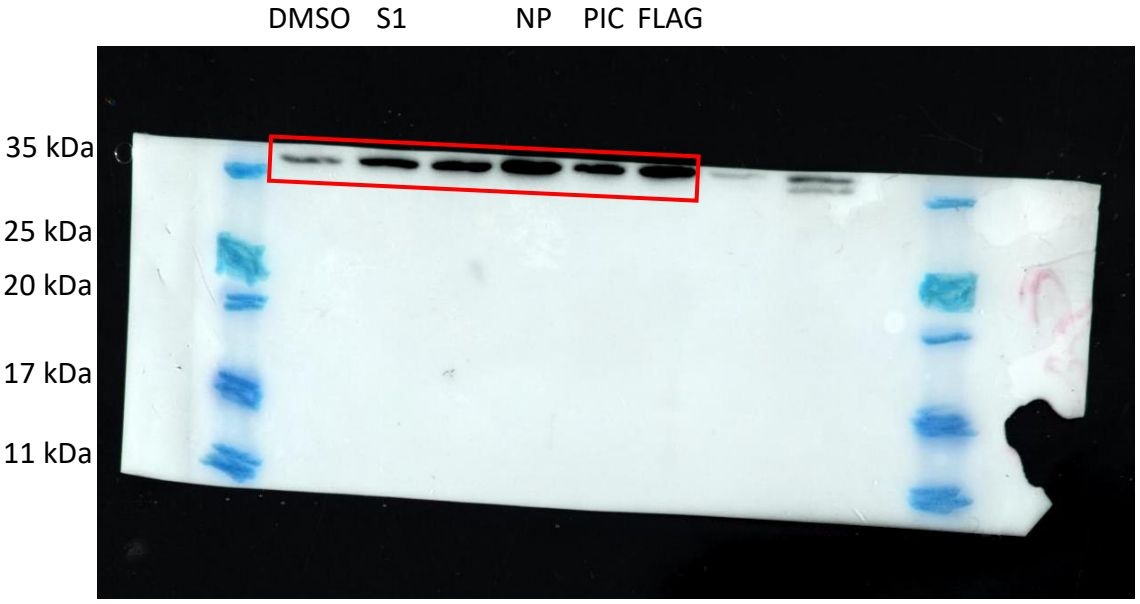

GAPDH (35 kDa) (FF26A/F9 BioLegend)

Chemiluminiscence+Marker

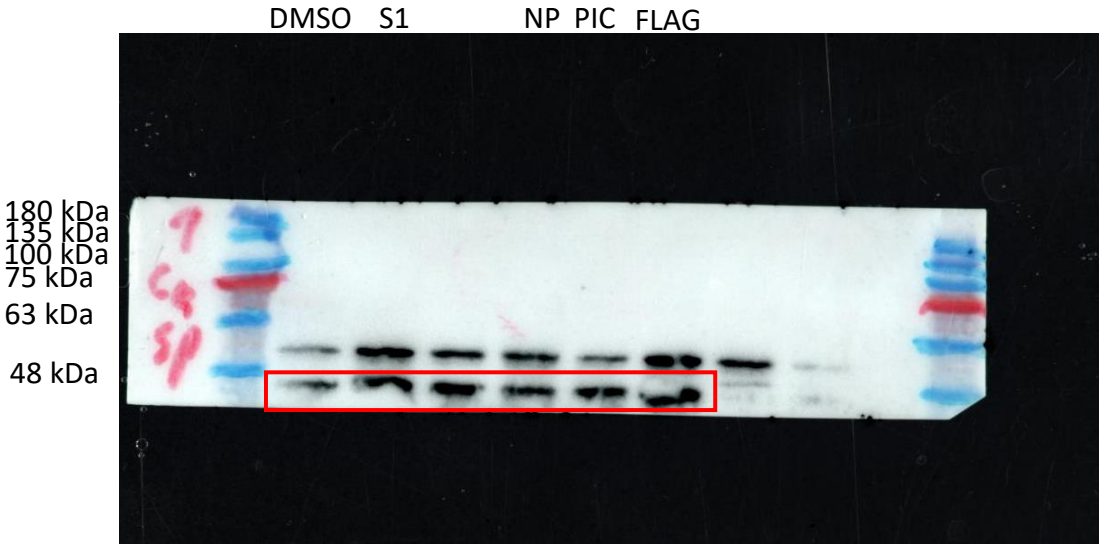

Chemiluminiscence

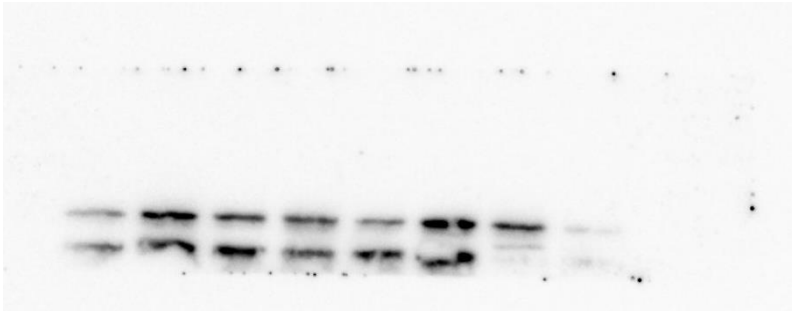

Caspase-1 and GAPDH included in Main figure 2C analysis

Cleaved Caspase-1 (52 kDa) (AF6215; R&D Systems)

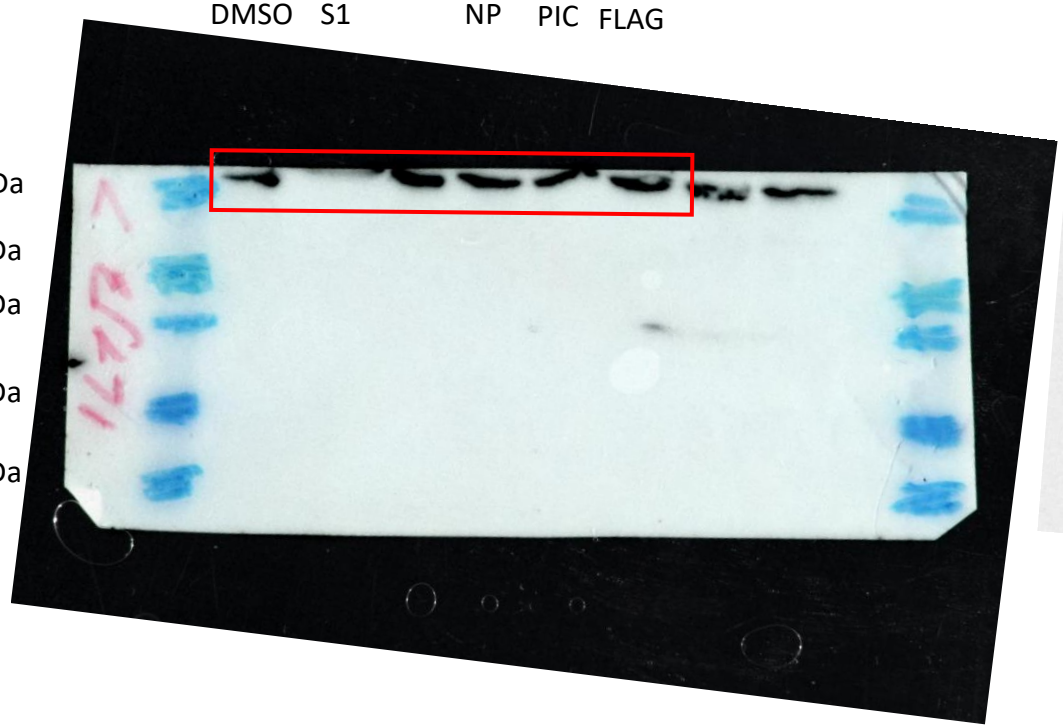

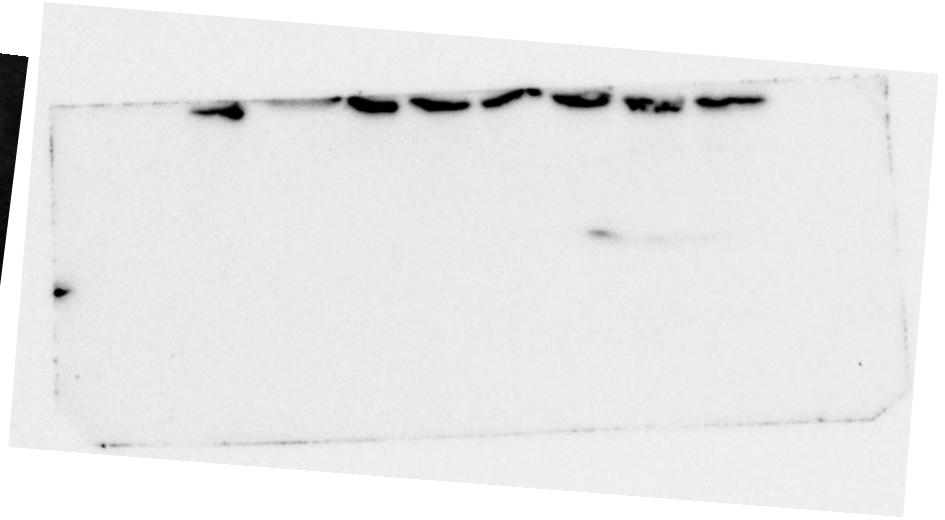

GAPDH (35 kDa) (FF26A/F9 BioLegend)

Chemiluminiscence+Marker

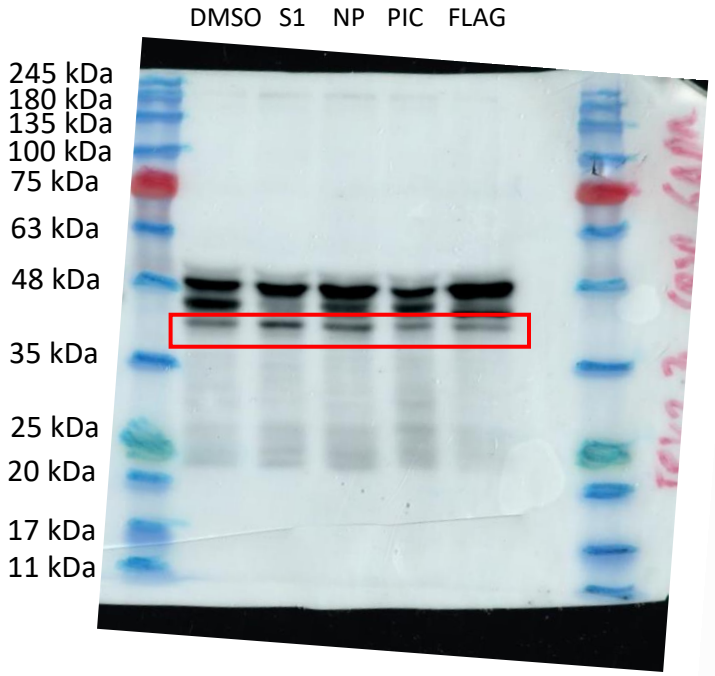

Chemiluminiscence

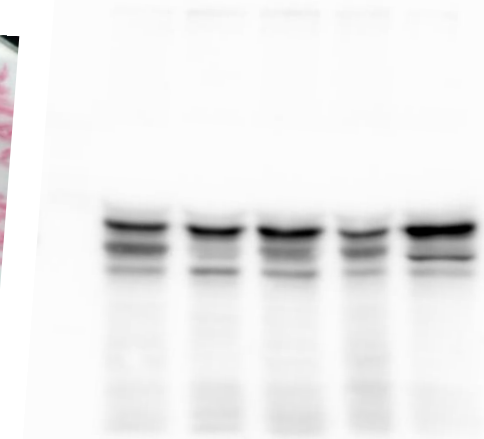

Cleaved Caspase-1 (52 kDa) (AF6215; R&D Systems)

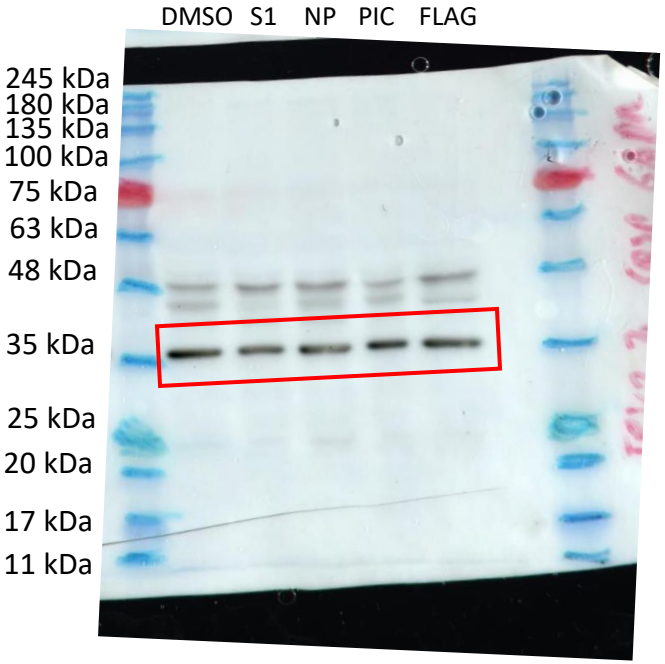

GAPDH (35 kDa) (FF26A/F9 BioLegend)

Caspase-1 and GAPDH included in Main figure 2C analysis

Chemiluminiscence+Marker

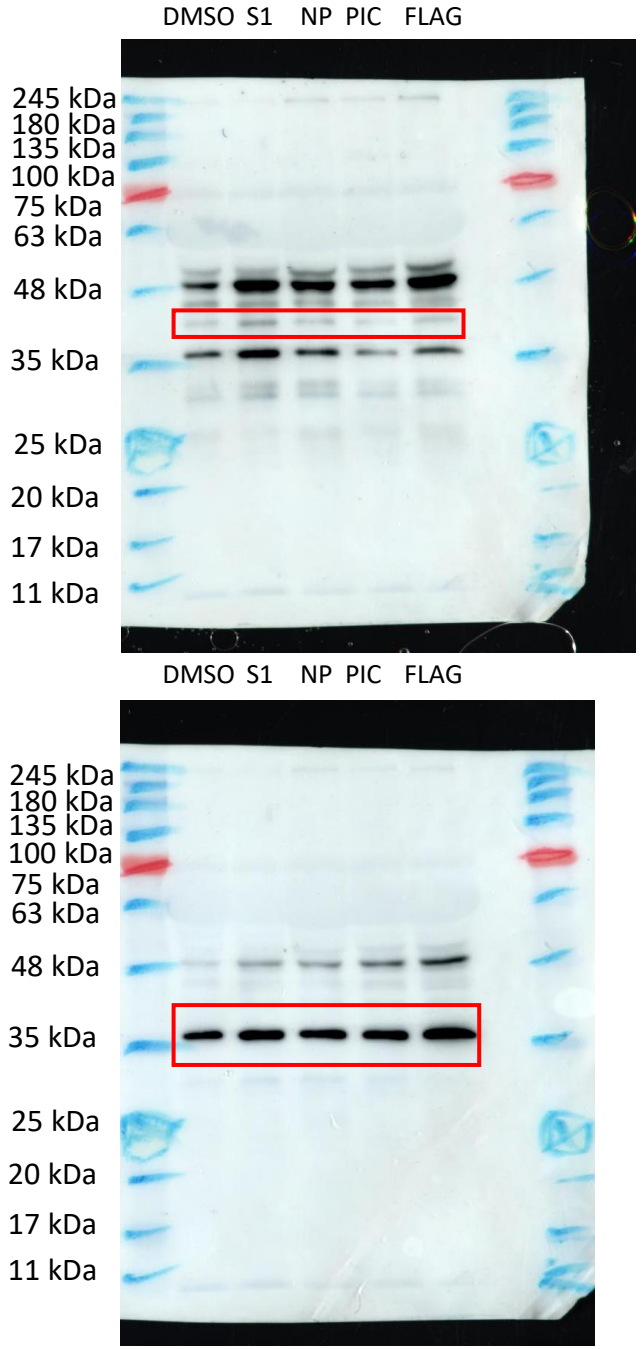

Chemiluminiscence

Cleaved Caspase-1 (52 kDa) (AF6215; R&D Systems)

GAPDH (35 kDa) (FF26A/F9 BioLegend)

Caspase-1 and GAPDH included in Main figure 2C analysis

Chemiluminiscence+Marker

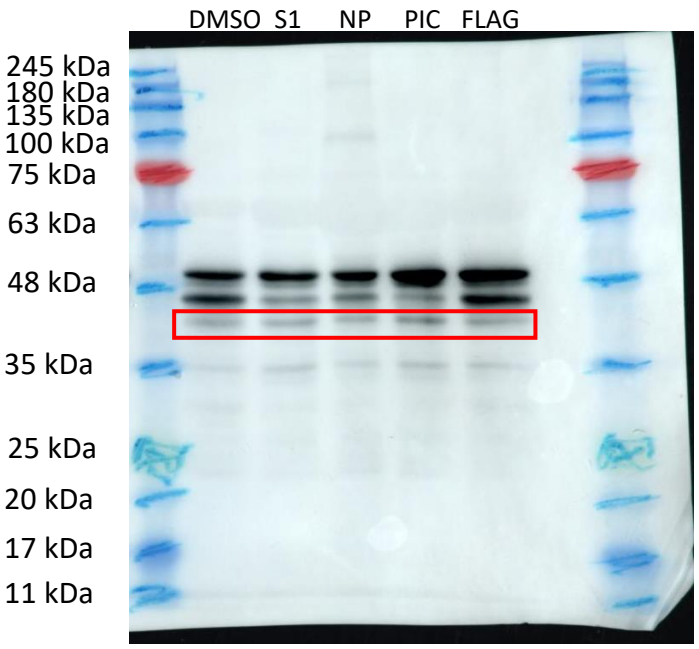

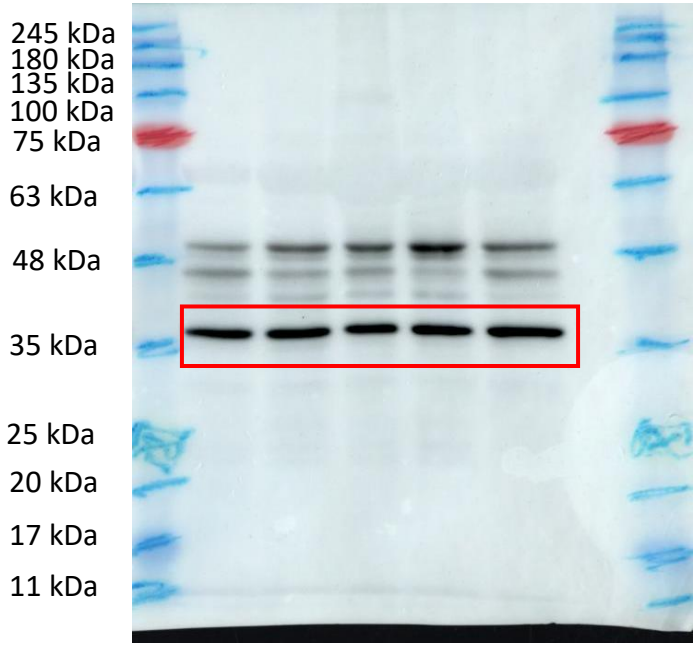

Chemiluminiscence

Cleaved Caspase-1 (52 kDa) (AF6215; R&D Systems)

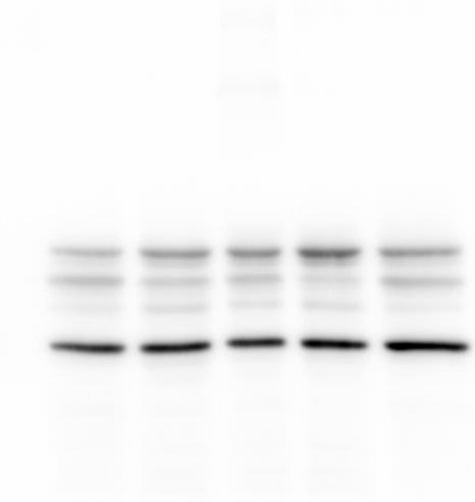

GAPDH (35 kDa) (FF26A/F9 BioLegend)

Caspase-1 and GAPDH included in Main figure 2C analysis

Chemiluminiscence+Marker

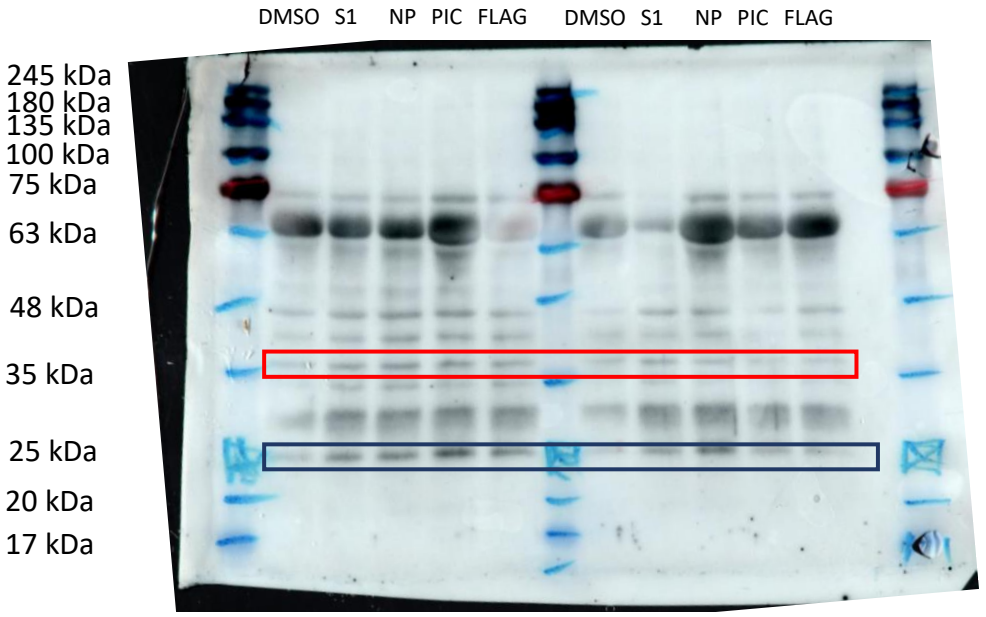

Chemiluminiscence

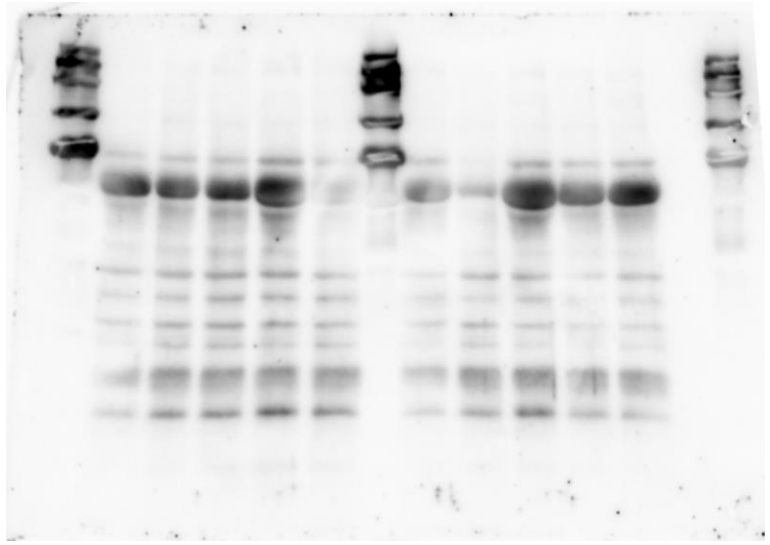

IL-1β and GAPDH included in Supplemental figure 2C analysis

IL-1β (31 kDa) (3A6, Cell Signaling)

Processed IL-1β (17 kDa) (3A6, Cell Signaling)

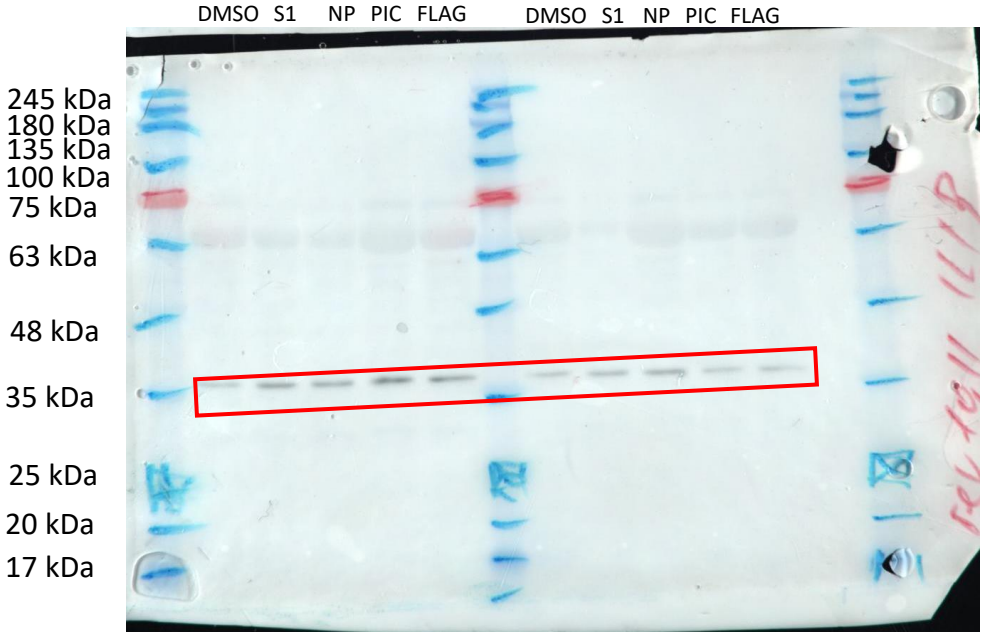

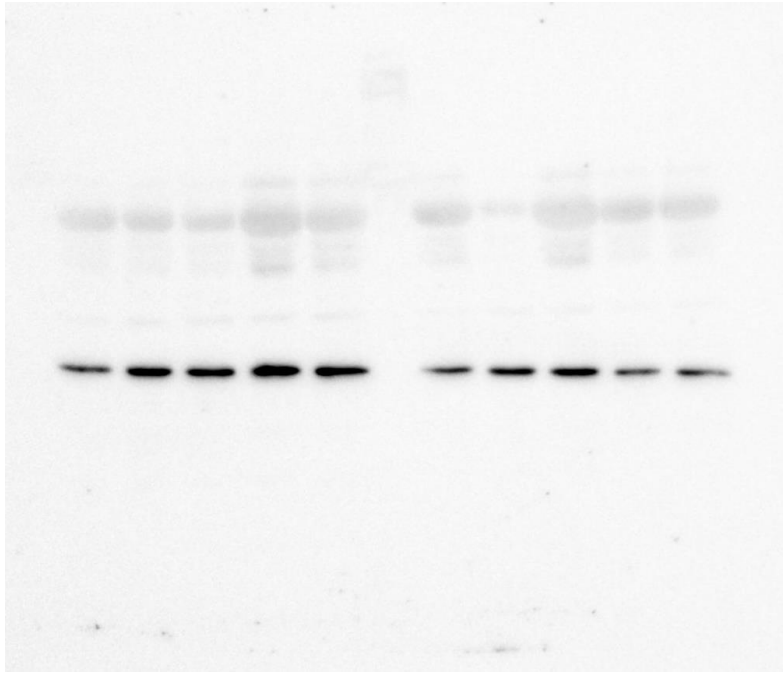

GAPDH (35 kDa) (FF26A/F9 BioLegend)

Chemiluminiscence+Marker

Chemiluminiscence

IL-1β and GAPDH included in Supplemental figure 2C analysis

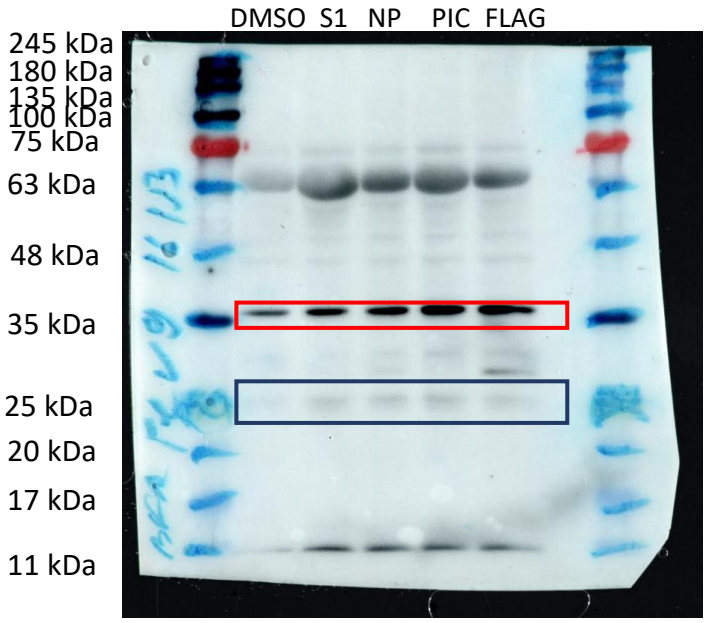

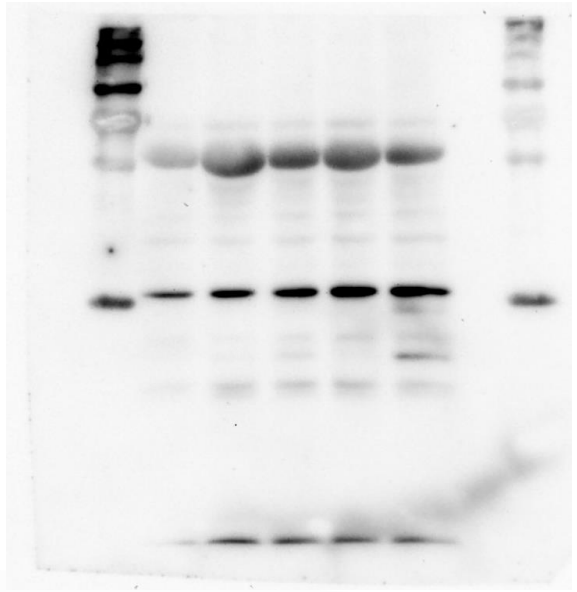

IL-1β (31 kDa) (3A6, Cell Signaling)

Processed IL-1β (17 kDa) (3A6, Cell Signaling)

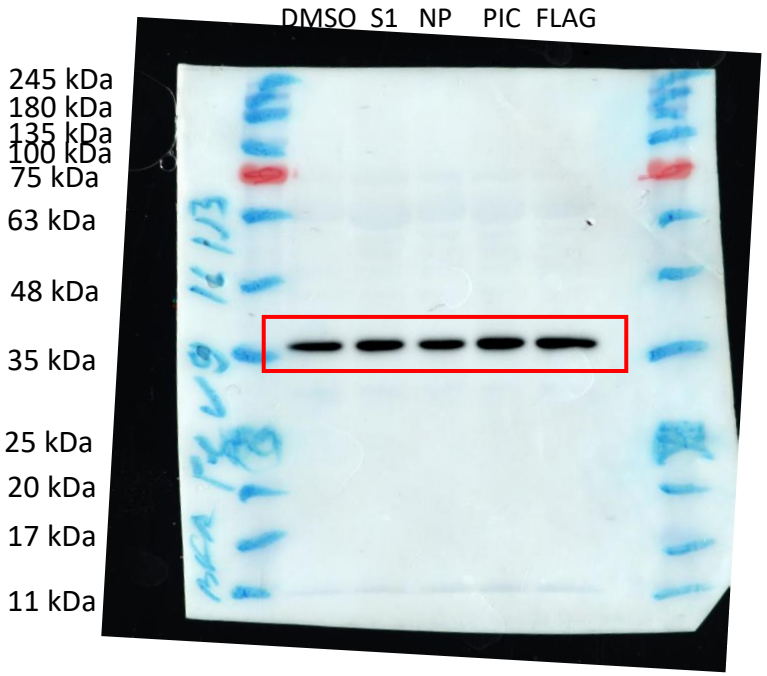

GAPDH (35 kDa) (FF26A/F9 BioLegend)

Chemiluminiscence+Marker

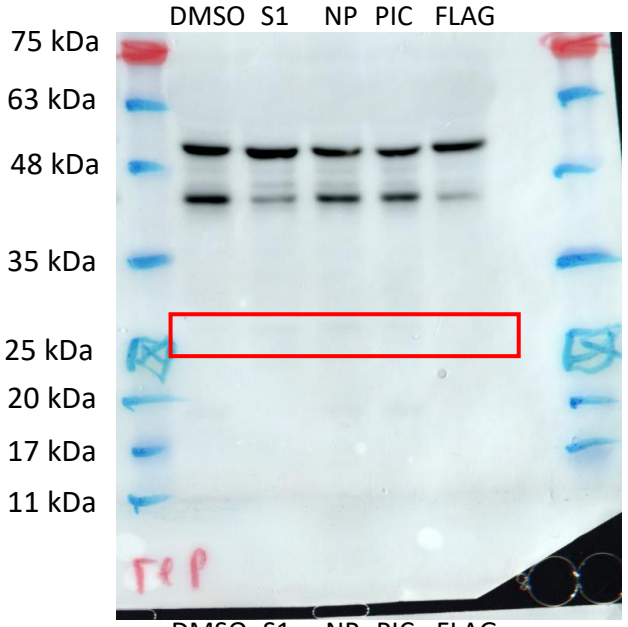

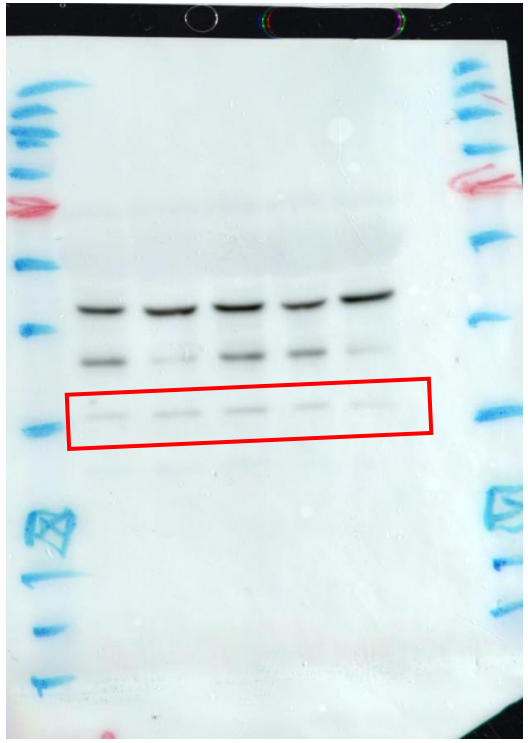

Chemiluminiscence

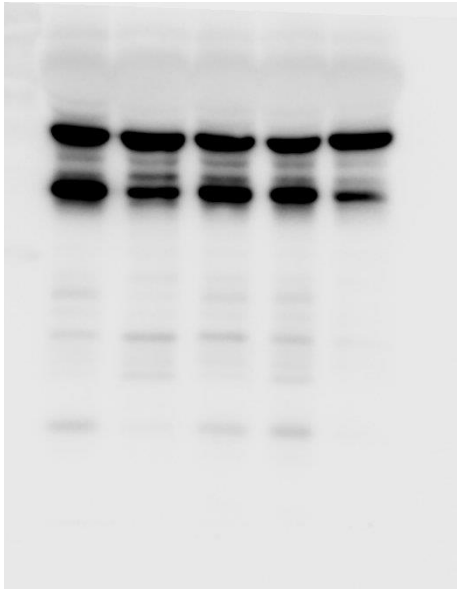

Cleaved Gasdermin D (21 kDa) (E5O4N, Cell Signaling)

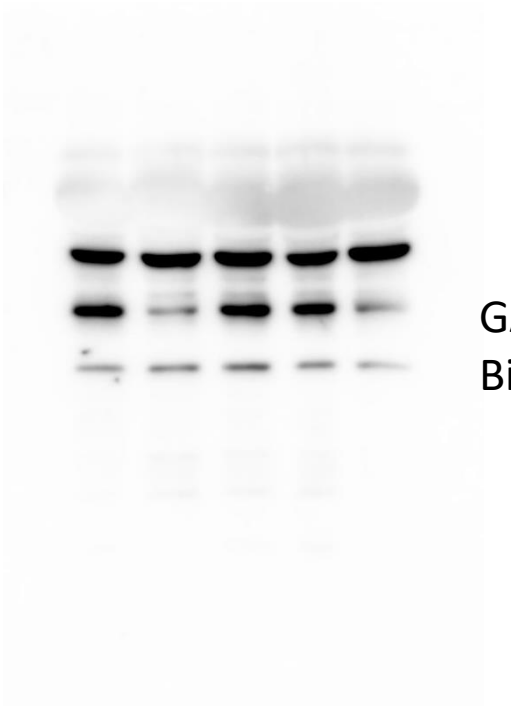

GAPDH (35 kDa) (FF26A/F9 BioLegend)

Gasdermin D and GAPDH included in Supplemental figure 2C analysis

Chemiluminiscence+Marker

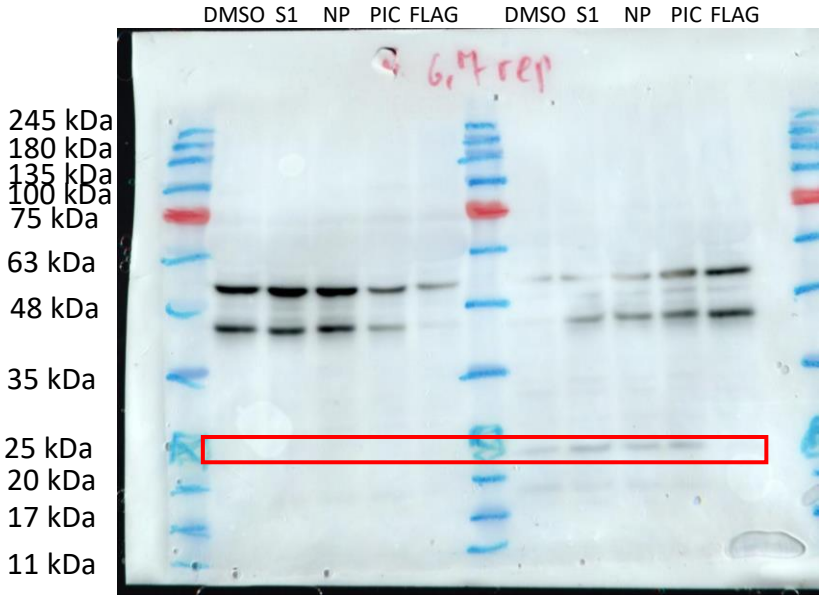

Chemiluminiscence

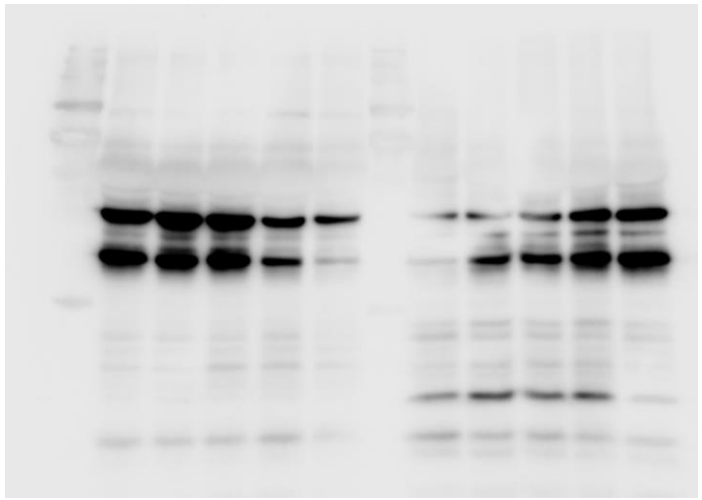

Gasdermin D and GAPDH included in Supplemental figure 2C analysis

Cleaved Gasdermin D (21 kDa) (E5O4N, Cell Signaling)

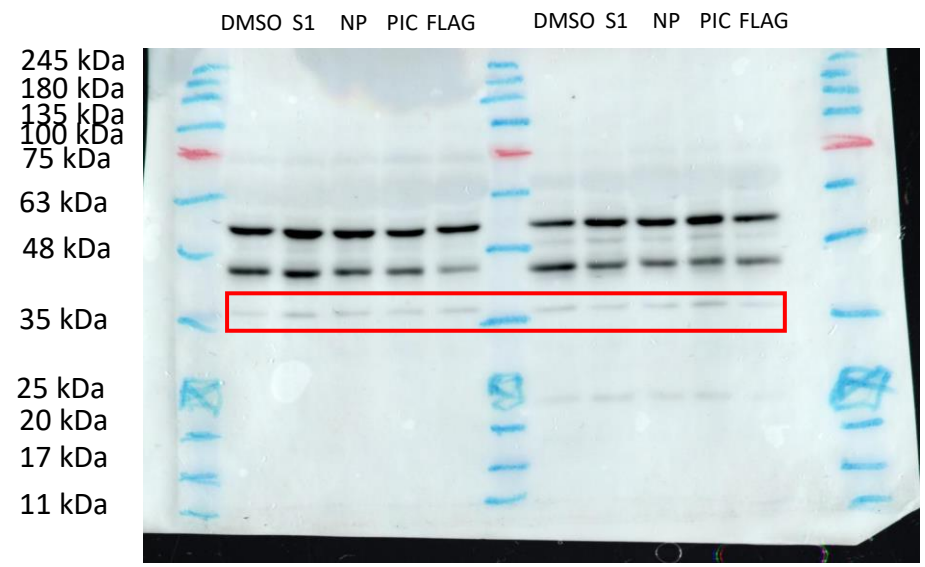

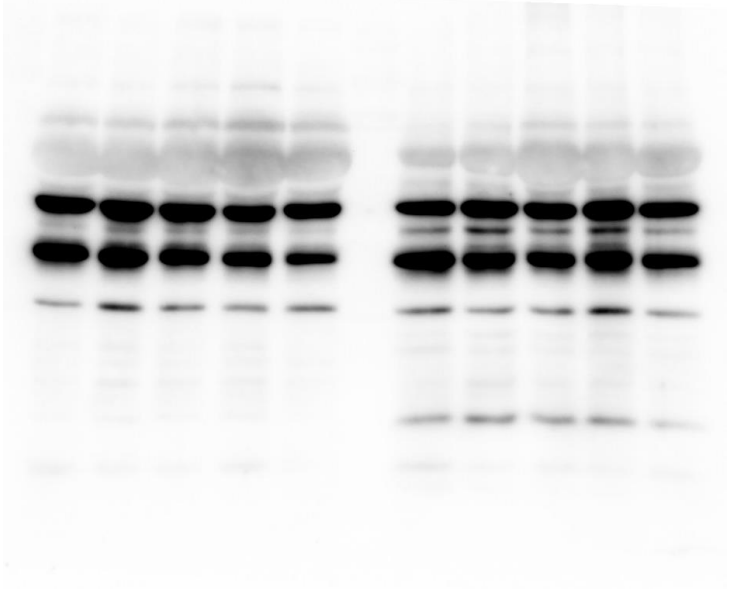

GAPDH (35 kDa) (FF26A/F9 BioLegend)